A review of in situ methodologies for investigating EHD contacts

Sayed Albahrani, David Philippon, Philippe Vergne, Jean-Marie Bluet

A review of in situ methodologies for studying elastohydrodynamic lubrication

SMB Albahrani[1], D Philippon[1], P Vergne[1] and JM Bluet[2]

Research in elastohydrodynamic lubrication (EHL) was, at its very beginning, essentially numerical, and even analytical. This area has, however, significantly evolved due to the necessity of validating the first models experimentally. Moreover, it soon became clear that the elastohydrodynamic (EHD) problem would be a topic of much more complex nature than the basic one involving perfectly smooth surfaces, Newtonian fluid, isothermal flow, etc. The experimental approach was the natural choice to make progress in offering the possibility of comparisons, first at the global level of the contact and, over time, at higher and higher spatial resolutions. The in situ analysis of elastohydrodynamic contacts was launched and everyone knows how much its contribution to the field has been and remains important. The present paper takes the task of reviewing the different in situ experimental techniques that have proven to be able to map the key-parameters in living EHD contacts. They are presented both in chronological order and according to the physical mechanism behind them, namely electrical, optical and acoustic methods. A last section presents some opportunities and recommendations for future works, with the aim to improve further our understanding of EHL.

Keywords
Elastohydrodynamic lubrication, experimental techniques, in situ mapping, film thickness or temperature or pressure distributions

Introduction

Elastohydrodynamic lubrication (EHL) was discovered through theoretical studies after the early work of Ertel in 1945,[1] and no quantitative experimental approach existed by then. It was not until 1950s that the first electrical techniques started to emerge. To date, different techniques have been developed and applied with more or less success. In parallel, the arrival of powerful computing resources and the development of specific numerical models have made possible the calculation, at any location within the film, of thickness, pressure, temperature and shear stress in elastohydrodynamic (EHD) contacts. In this context, it has been becoming necessary to compare and to validate the models with experiment. The agreement between the two approaches must be sought not only on global parameters, like central film thickness or friction, but also on the distribution over the whole contact area of the physical characteristics of the EHL regime as, for instance, film thickness, pressure, and temperature. From this dual methodology, it is possible to conduct a quantitative physics-based research on EHD lubrication.

In situ techniques naturally appear as the most interesting techniques to achieve this goal since they allow the investigation of the EHL regime under real conditions. However, their development is limited, or in other words rendered difficult by the extreme physical conditions that occur within EHD contacts. Some representative orders of magnitude are shown in Table 1 and typical pressure and film thickness distributions of an EHD contact are presented in Figure 1. Indeed these methodologies must be not perturbative to the phenomena under consideration to keep intact all the mechanisms that can occur in EHL. Moreover, considering the orders of magnitude reported in Table 1, other complex challenges lay in the required

[1]Université de Lyon, INSA-Lyon, CNRS, LaMCoS, UMR5259, F-69621, Villeurbanne, France
[2]Université de Lyon, INSA-Lyon, CNRS, INL, UMR5270, F-69621, Villeurbanne, France

Corresponding author:
P Vergne, Université de Lyon, INSA-Lyon, CNRS, LaMCoS, UMR5259, F-69621, Villeurbanne, France.
Email: philippe.vergne@insa-lyon.fr

Table 1. Typical orders of magnitude of the geometrical and physical characteristics in EHL.

Parameter	Order of magnitude
Film thickness	$< 0.5\,\mu m$
Contact zone diameter	$\approx 400\,\mu m$
Transit time of the lubricant in the contact	10^{-5}–10^{-3} s
Pressure	0.5–3 GPa
Temperature rise	Up to 100°C
Shear stress	Some kPa to some MPa

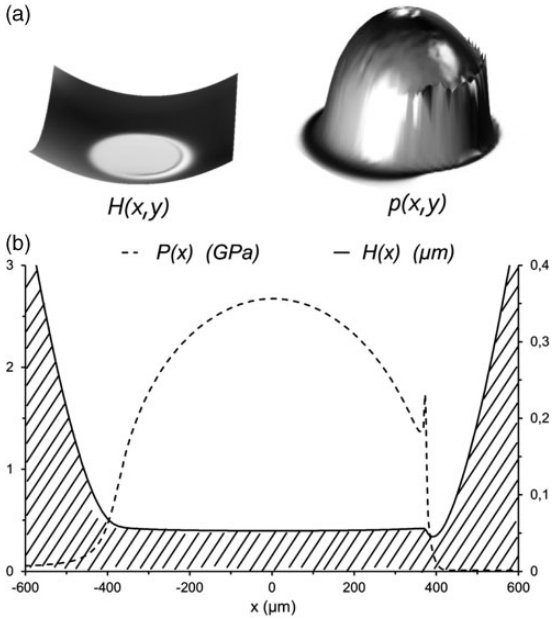

Figure 1. Typical pressure and film thickness distributions in an EHD contact: (a) pressure and film thickness 3D representations; (b) profiles along the contact central line (y=0) in the x-direction.

spatial resolution and in the extremely thin thickness of the material under investigation. Throughout the paper, an historical overview on the existing knowledge and the application of these techniques will be presented with more emphasis on recent developments that not only aim to probe key parameters but also to map them in EHD conjunctions. Generally speaking, these techniques can be subdivided into three categories depending on the directly measured parameter that is correlated to the sought characteristic in the EHD contact: electrical, optical and acoustic methods (as shown in Table 2). The content of the paper will follow the same order as presented in Table 2 to describe the *in situ* techniques and report their major achievements. This article aims to be as representative as possible of the field: due to the very large number of the papers published over the last 60 years it is, however, probably not fully exhaustive.

Electrical methods

Although optical methods are most widely used compared to electrical methods, they were historically preceded by electrical ones.[2] Electrical methods are applied to measure film shape and thickness, pressure and temperature. Different techniques have been developed in this purpose, such as voltage discharge, electrical resistance, and electrical capacitance.

Voltage discharge

Voltage discharge, alongside with electrical resistance, were applied in the 1950s and 1960s to measure film thickness in order to assess the validity of the available solutions of the EHD problem. The success was, however, moderate because of some difficulties encountered in the calibration processes prior to film thickness measurements in a genuine EHL regime.

Several authors used voltage discharge technique in EHL. Siripongse et al.[3] studied, in 1958, the relation between film thickness in line contact on one side and the voltage/current characteristics on the other side. MacConochie et al.[4] investigated, in 1960, the effect of load and oil viscosity on thickness variation of oil films formed between straight spur gears' teeth. Film thickness variations were measured between 2.5 and 10.2 μm, and were shown to be in the same order of magnitude in comparison with theoretical results. Using this technique Ibrahim et al.[5] studied, in 1963, the scuffing phenomena in gears.

In the previous works, calibration was the main obstacle to obtain reliable measurements. The relation between voltage discharge and film thickness was found to be linear, independent of the oil, but unfortunately very sensitive to surfaces' roughness and contact environment (presence of impurities for example). Later in 1966, Dyson[6] led a comparative study of film thickness measured using voltage discharge technique and the one obtained by an alternative method: electrical capacitance. Dyson found, as stated in the previous works, that there was some relation between discharge voltage and film thickness, but this relationship was far from being linear, since it was dependent on the slide/roll ratio and the temperature imposed or generated within the contact. The author concluded that this technique does not measure film thickness in the simple ways suggested before his work.

Electrical resistance

Film thickness and rate of metallic contact measurement. Measurement of film thickness is based on the proportionality of electrical resistance with film thickness between the rubbing surfaces. It was used in the beginning of its application to validate EHL solutions. It had been though a modest success. This is due to the complexity of electrical resistance variation within the contact, rendering difficult its calibration

Table 2. Past and recent *in situ* techniques applied to study EHD contacts.

Category of techniques	Technique	Measured parameter	First application in EHL
Electrical methods	Voltage discharge	Film thickness	1958
	Electrical resistance	Film thickness Rate of metallic interaction Temperature Pressure	1952
	Electrical capacitance	Film thickness	1958
Optical methods	X-rays	Film thickness	1961
	Optical interferometry	Film thickness	1962
	Infrared emission	Temperature	1974
	Infrared spectroscopy	Temperature	1975
	Raman spectroscopy	Pressure Temperature Film thickness	1983
	Fluorescence	Film thickness Lubricant flow	1974
Acoustic methods	Ultrasonic reflection	Film thickness	2003

with film thickness. However, when solid–solid contact happen to increase the severity of the contact, which may occur in many real engineering components, electrical resistance has been used relatively exclusively, due to its simplicity.[7,8] Measurement of film thickness is based on the proportionality of electrical resistance with film thickness between the rubbing surfaces. When a metal-on-metal contact occurs between surfaces' asperities, this resistance tends naturally to zero, whereas very high values are expected when a lubricant completely separates the two surfaces. This "discontinuous" resistance variation can be used as an indication of the degree of metallic asperities' interaction, and thus to establish the severity of a mixed lubrication regime.

The first work which applied electrical resistance for the purpose of evaluating film thickness was the investigation of Lane et al.,[9] in 1952, on gear lubrication. Electrical resistance values ranged from infinity to zero, and the authors expected that very small resistances (few ohms) were indicative of metallic contacts or of the presence of an extremely thin film of molecular dimensions. They, however, seemed to be cautious about determining absolute film thickness through the variation of electrical resistance. Firstly, because the conductivity of mineral oils varies quite rapidly with temperature and is affected by moisture and oxidation products present in some quantity in the experiments. Secondly, very thin oil films do not have necessarily the same electrical properties as bulk oil. The authors cited in particular the work of Needs,[10] in which it was showed that thin films begin to conduct at a thickness of 2.5 μm, and at 1.5 μm as well as a copper wire.

Furey[11] in 1961, and then Tallian[12] in 1964, were the first to apply electrical resistance in the quantification of the rate of metal-to-metal contacts in the mixed regime. Furey developed a device to study metallic contacts and friction between sliding lubricated surfaces, in which a fixed metal ball was loaded against a rotating cylinder. The values of both the instantaneous and the average electrical resistance between the two surfaces were measured. The instantaneous resistance value was used, as in Lane's work, to detect the transition between metallic contacts to full oil separation, and the average resistance was used as a measure of the percentage of the time that metallic contact occurs. Tallian et al.[12] adapted Furey's technique for a four-ball tester and could observe the existence and interruptions of EHD films through the variation of electrical resistance.

In 1983, Palacios et al.[13] conducted experiments with a four-ball tester to study the influence of surface roughness on oil films formation and their evolution during running-in. This influence was described by the parameter h/σ_h, where h is the film thickness and σ_h is the composite r.m.s. roughness determined by correlating the out-of-contact roughness measured via a stylus apparatus, and the frequency of metallic contacts measured by the variation of electrical resistance. The authors could show in particular that rough surfaces make thinner films than smooth ones (in which film thickness can be predicted by classical EHD theory), but if the above-mentioned parameter was larger than 2, roughness will have only a negligible effect.

Temperature and pressure measurement. Electrical resistance has been also applied to temperature and pressure estimation along the contact. The technique derives advantage from the electrical resistance sensitivity of some materials to temperature or pressure

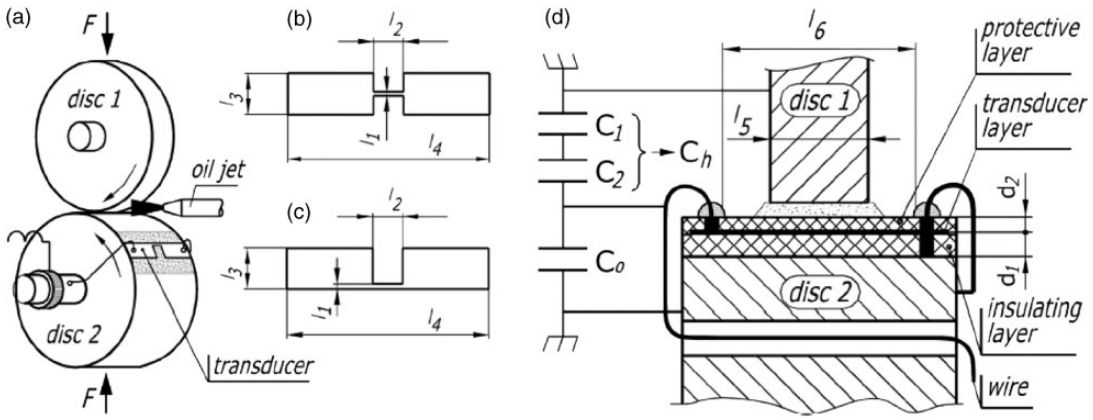

Figure 2. Design of a thin-layer sensor: (a) sensor in the two-disk system; (b) symmetric transducer; (c) asymmetric transducer; (d) cross section of the sensor. Published by ASME, Figure 2 from Wilczek.[23]

variations. A transducer, manufactured with appropriate materials, is deposited on one of the rubbing surfaces and in this way, after some suitable calibrations, one can measure temperature or pressure by monitoring the variation of its electrical resistance when it passes in the contact.

A pressure transducer is usually made of manganin (an alloy of Cu–Mn–Ni), and a temperature transducer is, in turn, made of titanium or platinum. These choices are due to the high sensitivity of manganin to pressure while being weakly sensitive to temperature, and to the high sensitivity of titanium or platinum to temperature while being weakly sensitive to pressure. The sensitivity to one parameter rather than both allows, in principle, for an accurate measurement of the variable of interest, by eliminating the error induced by the influence of the other one.

These thin-layer sensors are generally deposited using vacuum techniques, and they typically consist of three layers: (i) an isolating layer, which is directly deposited on the mating surface, (ii) a suitably shaped layer of a metal transducer, and (iii) a protective insulating layer made of aluminum oxide (Al_2O_3) or silicon oxide (SiO). Figure 2(a) to (d) shows a schematic of a thin-layer sensor deposited on one of the mating surfaces, its two common shapes (symmetric and asymmetric), and a cross section of it in which the different layers can be distinguished. The thin-layer sensor contraction is actually the active zone, and the two wide parts are nothing else than electrical leads.

Kannel et al.[14] reported for the first time in 1964 on the use of electrical manganin transducers for measuring pressure profiles in EHD contacts. They found that their measurements were reasonably reproducible and consistent.

Next year, Cheng and Orcutt[15,16] used separately a manganin resistance gauge and a platinum resistance gauge to measure pressure and temperature, respectively, within lubricated cylindrical disks under rolling and rolling-sliding conditions. The spatial resolution was quite low and consequently, the sharp pressure peak predicted by the theory at the contact outlet was not observed. The resolution was, nevertheless, sufficient to give some hint on its existence from the discontinuity in the pressure slope in that region. Under rolling-sliding conditions, results were compared with the most accurate EHD model available that included thermal effects, and some improved analysis of the inlet region and lubricant rheological model were suggested based on these comparisons.

In 1971, Hamilton and Moore[17] used an evaporated manganin gauge to measure EHD pressure. The active region was of the order of 0.5 mm long × 0.04 mm wide, and this allowed them to confirm the theoretical existence of a pressure spike near to the outlet. The peak was found in the correct position, but it was attenuated to some extent (Figure 3). Later in 1982, Safa et al.[18] developed thin-film manganin pressure transducers, sufficiently small (with an active region of 1 μm width) to allow the resolution of the pressure spike. In addition, they used the pressure transducer in combination with a temperature titanium transducer, developed by Kannel and Dow[19] in 1980, to correct pressure influence on temperature measurements. This transducer consisted of a titanium thin-film temperature sensor deposited on top of a manganin thin-film pressure sensor. Indeed, thin film titanium (unlike bulk titanium) was found to have a pressure sensitivity sufficiently large to induce error in temperature reading. Clearly, this means that titanium thin-film pressure coefficient has to be preliminarily calibrated, so that the part of the change in resistance due to temperature rise could be determined with an acceptable confidence.

These were some pioneering examples of works on the application of electrical resistance to the temperature and pressure mapping in EHL. The transducers, or in certain cases microtransducers, began to become widely employed in the 1980s. Later on in the 1990s

they became almost routinely used, thanks to modern electronics and possibilities of miniaturization.[7]

In 2006, Höhn et al.[20] studied the influence of surface roughness on pressure distribution occurring in a twin-disk test rig. For this purpose, the authors investigated different surfaces on top of which they deposited, using a sputtering device, a thin film sensor made of manganin. The authors could, for instance, measure pressure profiles on polished surfaces. In order to prevent any damage of the sensors, the study was restricted to pure rolling conditions and to film minimal thickness ranging between 2.5 and 3.5 μm, which is not really representative of the encountered film thicknesses in EHL.

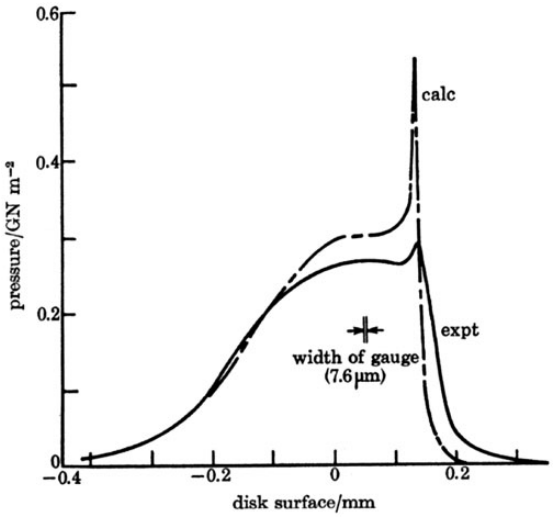

Figure 3. Comparison between theoretical and experimental pressure distribution. Reproduced with permission of the Royal Society from Hamilton and Moore.[17]

In another experimental investigation conducted by the same group, Miyata et al.[21] measured for the first time temperature rise in elliptical contacts under high rolling speed and slight sliding conditions, such as those found in toroidal CVT. Temperature rise measurements were performed by means of a thin-film sensor made of platinum deposited over an Al_2O_3 insulating layer and applied to the disk steel surface (see Figure 4(a)). The platinum is, even in minute amount, sensitive to pressure. The sensor was thus calibrated both in temperature and pressure. Temperature calibration was performed in a controlled-temperature oil bath, whereas pressure calibration was carried out in the same twin-disk test rig, but under slow entrainment speed and zero-slip condition (guaranteeing in this way that no significant temperature rise would occur). An example of results is shown in Figure 4(b) in which temperature rise profile is plotted for different values of slip. Considering all the influencing factors, the authors assigned an overall relative error of 8% to temperature rise measurements.

As it can be noticed from the two last studies, the spatial resolution was limited by the dimensions of the active part of the microtransducers. Their width ranged between 5 and 35 μm, and their length between 0.25 and 1.5 mm. Temperature or pressure were thus averaged over these dimensions. This is well adapted for linear or elliptical contacts (with the major axis oriented perpendicular to the entrainment speed) where profiles along the central axis can be obtained. However in point contacts were the diameter of the contact is ~400 μm, the resolution is no more satisfactory and thus mapping temperature or pressure is no longer possible.

Application of electrical resistance to measure temperature and pressure in EHL contact has been quite extensively developed since 1960. However, this

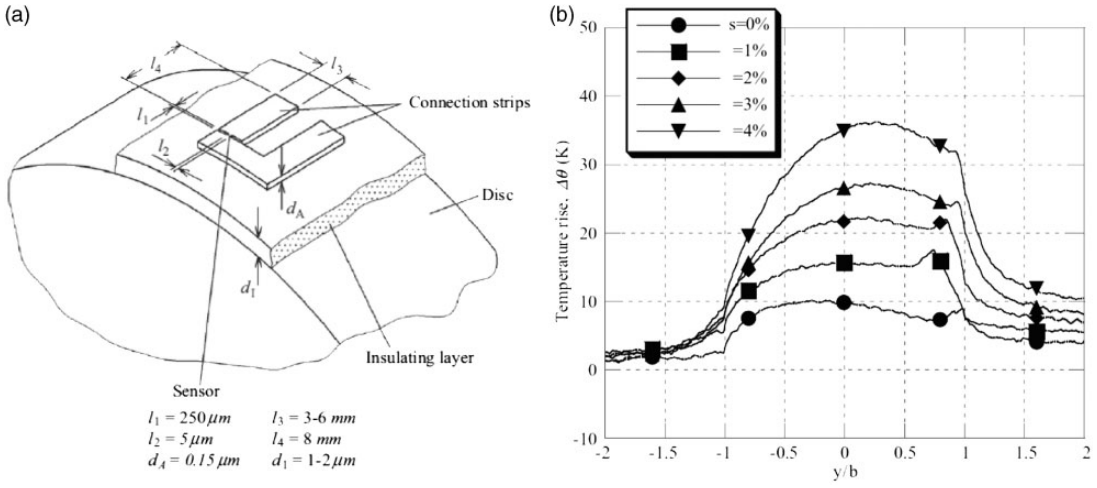

Figure 4. (a) Platinum temperature sensor; (b) Temperature rise along the center line in rolling-sliding-spinning conditions. Reproduced with permission of Elsevier from Miyata et al.[21]

technique presents some disadvantages or limitations, especially those discussed in the paper of Marginson et al.[22] The authors introduced a new strain-related model (that they could verify experimentally) of the response of the transducers within the contact due to the rise of temperature. This model had, according to the authors, some profound implications on the results obtained from this type of transducers. The most important are the followings:

- Stress/strain regime encountered in an EHD contact can have some influence on the response of the gauge and this implies that calibrations must be conducted in the same stress/strain regime to get reliable results.
- Small variation of the mechanical properties during gauge fabrication, relatively to those of the bulk material, can have an important effect upon the sensor response. This is actually the case since the thin-film gauge do not have the same properties as the bulk material and, moreover, these properties depend upon manufacturing processes.
- A significant proportion of temperature rise reading can arise from the strain encountered by thermal expansion of the insulating layer within the contact, while temperature calibration gives simply and only the intrinsic temperature coefficient of the electrical resistance of the transducer.

Additional difficulties exist, some of which were mentioned in the presentation of previous works:

- The zero sensitivity of titanium or platinum to pressure is not anymore valid.
- The purity of the lubricant is a common default of electrical methods since the passage of the electrical current through the lubricant is greatly influenced by the presence, nature and size of impurities.
- Transducer thickness has to be extremely low (between 0.03 and 0.15 μm) in order to reduce its influence of the lubricant flow within the contact. Since this effect cannot be completely eliminated, the technique is to some extent intrusive regarding the typical EHL film thickness range.
- Lifetime of deposited transducers is a major issue because of the severity of the operating conditions in EHD contacts. The presence of sliding between the rubbing surfaces makes the situation worse and, whenever this happens, lifetime is considerably reduced. This signifies that the technique is limited to pure rolling or, at best, to only relatively small sliding conditions.

Recently, in 2011 and 2012, Wilczek[23,24] conducted theoretical and experimental studies on the influence of some additional parameters on the accuracy of pressure measurement in EHD line contacts using electrical resistance. Herein, two interesting implications and/or recommendation are mentioned:

- Thin-layer sensor design, and its shape in particular, can have a significant influence on the accuracy of the measurements. For example, an asymmetric transducer affects much more significantly the measurement accuracy than symmetric ones, and the latter were proved to be optimal.
- Measurement accuracy can be improved by reducing the resistance and capacitance of the sensor, and increasing its pressure coefficient of resistance.

It could be noted from the description of different works on the technique that its main advantage is its applicability to contacts formed between two metallic bodies. This allows, in particular, for the investigation of temperature and pressure conditions experienced in real machine components. As we will discuss it later, this is not a common feature between the different *in situ* experimental methods used in EHL. Optical methods, namely, require one of the surfaces to be transparent to the employed radiations.

Electrical capacitance

Electrical capacitance technique was developed in the end of the 1950s, and it became widely used in the study of EHL. It confirmed, alongside with optical interferometry, EHD theory predictions with respect to the film thickness shape, and its dependence upon operating conditions and lubricant rheology.[7] This technique is based on the measurement of the electrical capacitance between the rubbing surfaces, considering each one of them as a part of an electrical capacitor (Figure 5(left)). As the capacitance is directly related to the distance between surfaces, this technique can be applied to measure film thickness. For calibration purposes, parallel-plate capacitor approximation can be used[2]

$$C = \varepsilon_0 \varepsilon_r \frac{A}{h} \tag{1}$$

where C is the capacitance for two parallel conducting metallic plates of area, A, separated by a material with dielectric constant, ε_r, of a thickness, h, and ε_0 is the dielectric constant of vacuum. This formula has two important implications:

- The less is film thickness, the more important will be the detected electrical capacitance, and this makes electrical capacitance suitable for studying thin films.[2]
- The accuracy of electrical capacitance method rests upon the knowledge of the dielectric properties of the lubricant and its variation with temperature, pressure and other influencing factors.

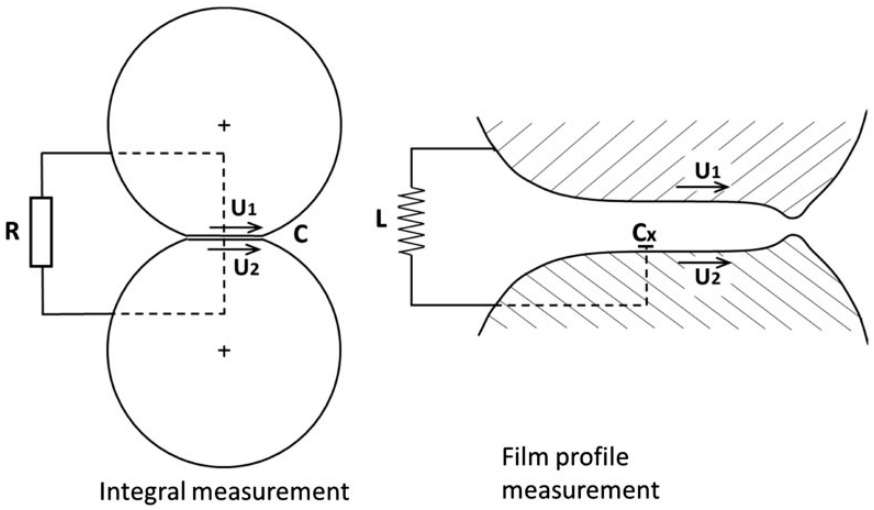

Figure 5. Application of electrical capacitance method to measure the mean film thickness (left) or the film thickness profile (right).

In order to gain in resolution, a microtransducer can be deposited on one of the surfaces. In this case, the electrical capacitance variation between the microtransducer and the other surface is monitored while the former (noted *Cx* in Figure 5(right)) passes across the contact.

Electrical capacitance technique was initially developed by Crook[25] in 1958, who evaluated EHD film thickness in the contact between two parallel lubricated disks. The motivation behind this new method was the fact that the only technique available by then, i.e. voltage discharge, suffered from an important weakness: it attributed to the oil film under a genuine contact the electrical behavior observed in a static calibration experiment where greatly different physical conditions can be experienced. Electrical capacitance method does not suffer, to the same extent, from this weakness since it relies only upon dielectric constant of the oil, which is essentially a function of pressure and temperature within the contact. Prior to film thickness measurements using electrical capacitance, Crook made use of unloaded contacts between the disks and stationary pads to perform his calibration. This choice was made in order to avoid additional errors induced when the true shape of the contacting surfaces was not used during the calibration.

In 1961, Crook[26] developed his own technique and used microtransducers to measure film thickness. This improved, as mentioned above, the resolving power of the measurements. The contact under investigation was formed between two disks, one of which was of glass and carried the evaporated chromium electrode, and the other was made of hardened steel. A typical result can be seen in Figure 6, in which the potential (proportional to ε/h) is found to vary as a function of the time and thus represents film thickness across the contact. The parallel section in the middle, in which film thickness is about 1 μm, and the existence of a

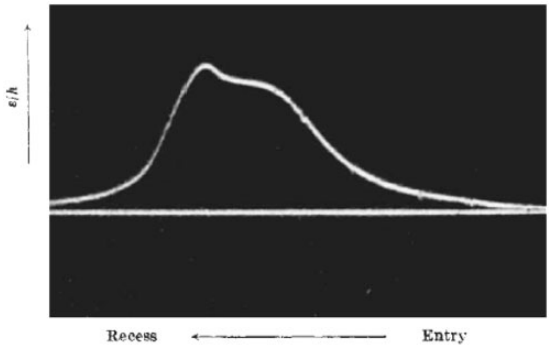

Figure 6. Oscilloscope trace (representing the inverse of film thickness) as a function of time. Reproduced with permission of Macmillan Publishers Ltd from Crook.[26]

constriction, in which film thickness falls by approximately 10%, could confirm quantitatively the theoretical features predicted by Dowson and Higginson[27] and Archard et al.[28]

Dyson and Wilson[29] pursued the validity assessment of EHL theory predictions, especially those of Dowson and Higginson.[27] They compared the predictions with measurements obtained with a twin-disk machine lubricated with a wide variety of lubricants, and close agreement was found over the range 0.03–1 μm for most of the tested fluids.

Hamilton and Moore[30] designed, in 1974, a very small flat capacitive gauge (of 1.25 mm in diameter) adapted to the conditions of a working engine in order to evaluate film thickness between a piston ring and the cylinder. The authors could observe film thicknesses in the range 0.4–2.5 μm under different conditions of speed, load, and temperature.

In the years following these first developments, electrical capacitance technique has been employed in various applications. For instance, Wilson[31] carried

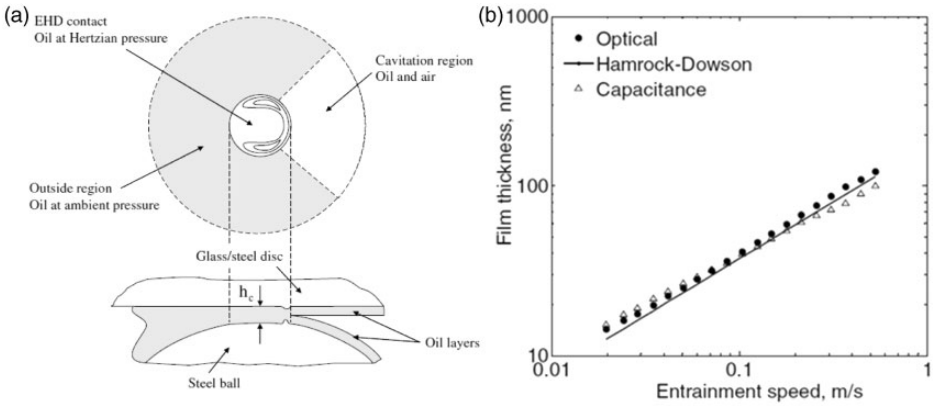

Figure 7. Capacitance measurement: (a) schematic indicating the Hertzian contact area, the outside of contact region, and the assumed spatial distribution of oil around; (b) example of agreement between theoretical and experimental film thickness measurements (using a chromium-coated glass disc). Reproduced with permission of IOP Publishing from Jablonka et al.[2]

out, in 1979, a comprehensive study on grease film formation between the rollers and the rings of rolling element bearings. Thinning of grease films was observed, and attributed to partial starvation. Another application was conducted by Sherrington and Smith[32] in 1985 on a low-pressure system. The authors performed film thickness measurements between a piston ring and the cylinder, and they designed accordingly a capacitive transducer which could generate a signal proportional to the gap separating the two bodies.

More recently, Chua et al.[33] measured dynamic thickness of organic films between sliding metallic surfaces. The experimental setup was a ball-on-disk tribometer. Film thickness was measured using the parallel-plate capacitor formula, in which the real contact area of the contact was taken into account. This latter area is proportional to the load and the apparent surface area for a given constant surface roughness. The authors discussed the factors that could affect the measurement accuracy through their influence on the dielectric constant of the film, mainly:

- The presence of water in the contact.
- The change in the molecular structure of the boundary film, especially during sliding, by means of tribochemical reactions.
- The adsorption onto the surface of species of a different chemical nature from the bulk fluid, such as additives.
- The polarization of the boundary film due to capacitance generation between the metallic surfaces.

The correct evaluation of the real contact area is also crucial, and the assumption of this area being independent of sliding, as it was made by the authors, is not valid under excessive wear and could generate erroneous film thickness estimations. This was not a concern in that study since the oil film was relatively thick, in such case significant wear is not likely to occur.

In 2012, Jablonka et al.[2] used a new approach to extract thin film thickness from the measurement of electrical capacitance. They first applied this approach simultaneously with optical interferometry technique using a steel ball loaded on a chromium-coated glass disk. Subsequently, a steel-on-steel contact was studied where optical interferometry is no longer applicable. In this approach, the measured capacitance, C_{tot}, was regarded as the sum of the capacitance of the Hertzian contact, $C_{contact}$, that of the region outside the contact, C_{out}, and finally a background capacitance as shown in Figure 7(a). The background capacitance was evaluated by measuring the capacitance of the system without the ball connected and was found to be negligible. The outside of the contact capacitance was calculated after dividing it into two regions: the flooded and the cavitated regions (Figure 7(a)). The capacities in both regions depend on the profile of the deformed surfaces outside the contact and also on film thickness within the contact. The former was estimated based on Hertz's theory, and the latter was either measured by optical interferometry or calculated by Hamrock–Dowson equation (depending on the disk being used). The contact capacitance was next evaluated by simply subtracting the outside capacitance from the total measured capacitance, and it was finally converted into film thickness by assuming a parallel-plate geometry approximation. Using this procedure the authors found, for the investigated lubricants, film thicknesses in good agreement with the ones measured by optical interferometry or predicted by Hamrock–Dowson formula in the range between 15 and 200 nm (see Figure 7(b)).

Jablonka et al.[34] completed their work using the same approach to study the influence of the lubricant's polarity on the accuracy of capacitance measurements, and this by using liquids of different

polarities. For polar liquids, the film thickness derived from electrical capacitance deviated from the one measured optically. The authors suggested a three-layer model taking into account the formation of a "dead-layer" by adsorption of the polar liquid molecules on the contacting surfaces. This layer leads to a lower polarizability of the lubricant within the contact and thus smaller effective dielectric constant which decreases, in turn, the measured capacitance and results in an overestimated film thickness. This study showed, inter alia, that it is possible to get a more complete picture of the behavior of the lubricant in thin films by combining electrical and optical methods.

In short, as it can be noted from the description of the different papers on film thickness measurement using electrical capacitance, two main trends are still persisting. The first one consists in measuring the electrical capacitance between the surfaces in contact, and the other in measuring it between an electrode, deposited on one of the surfaces, and its counterface. Although the first trend suffers from a lower spatial resolution, it has the advantage of not being as vulnerable with regard to the severity of the contact as the second one.

Optical methods

In the following, optical methods must be considered in a broad sense, thus covering a significant part of the electromagnetic spectrum, i.e. from X-rays to infrared and, in between, visible radiations. When necessary, and especially for specific techniques that are not in routine use in lubrication, a brief description of the underlying physical phenomena will be provided.

X-ray transmission

X-ray transmission technique has been used a few times in the 1960s for film thickness measurement. It consists basically in measuring the amount of X-ray beam that passes through the lubricant within the contact when the latter is irradiated with collimated X-rays, provided that metallic bodies absorb largely such radiations whilst oils are essentially transparent to them.

This method was initially developed by Sibley and Orcutt[35] in 1961 to measure the thickness and shape of oil films formed between the surfaces of hardened steel rollers under rolling, or rolling and sliding conditions. To do so, a square, monochromatic beam of X-rays was directed at the contact parallel to the axes of rotation of the rollers, and then detected by a radiation counter at the rear of the rollers. Film thickness was obtained after calibrating disks centers' separation (measured with a dial indicator) with X-ray counts. Film thicknesses ranging between 0.1 and 1 μm were measured. Given the diameter of the X-ray beam, and the mechanical precision of the test-rig, film thickness profiles were obtained with a spatial resolution of 0.8 mm, and with an estimated accuracy of about 60 nm.

In 1965, Kannel et al.[14] used film thickness and disks deformation, measured via X-ray transmission technique, to infer pressure distributions in the contact formed between two rolling steel disks. Essentially the same technique was used as in Sibley's work[35] with some technical improvements. First, in order to improve by an order of magnitude the spatial resolution, the radiation passed through a 76.2 μm wide vertical slit before illuminating the contact. Second, X-ray count rate was calibrated by comparing the known profile of the disks in an unloaded static condition with the profile recorded by the transmitted X-ray radiation.

This method could never impose itself, and this is maybe because other techniques, much more simple, less expensive, and more powerful and accurate became able to measure film thickness, such as electrical capacitance, as described above, or optical interferometry, as we will discuss in next section.

Optical interferometry

Optical interferometry is undoubtedly the most powerful technique for *in situ* film thickness measurement, and even in EHL experimental research more generally. The major and almost unique constraint/drawback lies in the use of a transparent material which presents a perfectly smooth surface. Optical interferometry was initially developed by Kirk[36] in 1962, but the subsequent 30 or 40 years have witnessed the succession of many developments, which permitted the gain in resolution, measurement range and accuracy.

Conventional optical interferometry. When a lubricated contact, formed between a transparent disk (glass or sapphire) and a steel ball, is shone by a monochromatic light, the latter splits essentially into two beams of approximately equal intensities. One reflects at the glass–oil interface, and the other at the ball surface. These different optical paths results in interference of the two beams. Depending on the optical path difference (OPD) in a given point, which itself depends upon the separation between the ball and the disk at that point, this interference will be either completely or partially constructive or destructive. If the two beams after reflection are in phase, or equivalently the OPD is a multiple of light wavelength, this interference will be constructive, and destructive in the opposite case. However, the separation between the ball and the disk varies as a function of the two bodies' respective initial geometries and their deformation due to the different stresses within the contact. This leads to the formation of the so-called interference fringes with all their possible patterns as shown in Figure 8(a) and (b). These patterns can be

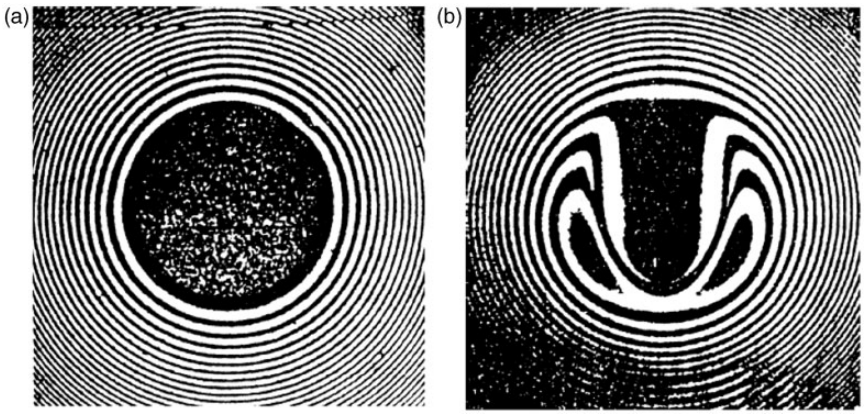

Figure 8. Interference fringes using monochromatic illumination under (a) static conditions, and (b) dynamic conditions, from Foord et al.[37] Reproduced with the permission of the Institution of Mechanical Engineers and SAGE Publications Ltd.

regarded as a contour map of film thickness, in which each iso-line represents a constant film thickness whose value can be determined by using appropriate formulas or after some calibrations.

In fact, if the illumination is monochromatic, as illustrated above, different formulas can be used, such as two-beam or multiple-beam interference equations. Conversely, if a chromatic beam is used, much more complicated physical and optical phenomena occur, which can be roughly regarded as some kind of combination of interference processes of each wavelength, and no simple mathematical formula exists to describe it quantitatively. Naturally, the interference pattern, or the interferogram, will be colorful and film thickness determination will require some preliminary calibrations (under static condition for example). Chromatic illumination offers, however, a higher resolution in film thickness measurements.

Duochromatic illumination has been an alternative in order to obtain images with a better contrast and a measurement resolution comparable to that obtained with chromatic illumination.[37,38] Moreover, it provides an extended measuring range compared to chromatic interferometry and, for this reason, has been used to study the mechanisms responsible for the occurrence of dimples[39,40] in EHL. Table 3 compares the performances of conventional interferometry obtained when the different possible illuminations are used.

Optical interferometry was primarily developed in EHL to validate theory. Figure 9 shows one of the first comparisons between theoretical predictions and experimental results obtained by Cameron and Gohar[41] in 1966, using monochromatic light in contacts formed between a steel ball loaded against a fixed glass plate. In 1968, Foord et al.[42] improved the method in terms of fringes contrast. Actually transparent materials used for the disks (such as glass) have a refractive index approaching that of the lubricant. This leads to a relatively low light

Table 3. Comparison between the different modes of illumination for conventional interferometry.

Technique	Minimum thickness	Maximum thickness	Measurement resolution
Monochromatic	$\approx$ 50 nm	Several μm	$\approx$ 100 nm
Duochromatic	$\approx$ 50 nm	Several μm	$\approx$ 40 nm
Chromatic	$\approx$ 80 nm	1 μm	$\approx$ 40 nm

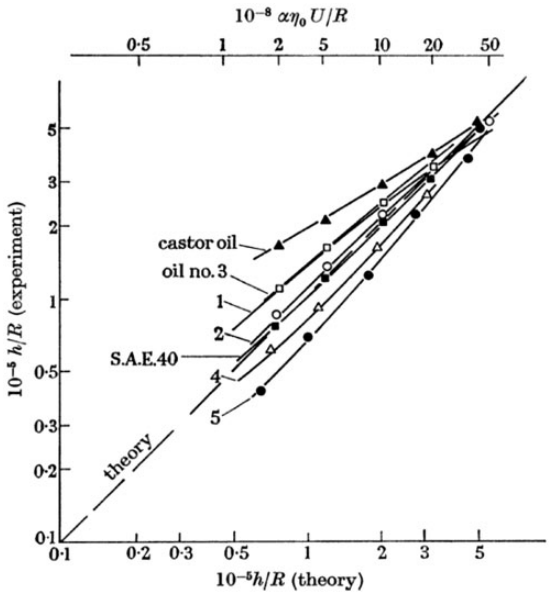

Figure 9. One of the first comparisons between theoretical predictions and experimental results from optical interferometry. Reproduced with permission of the Royal Society from Cameron and Gohar.[41]

reflection at the interface between the disk and the oil and, consequently, poor image contrast. In order to solve this problem, the authors introduced the use of semi-reflecting, 100 Å thick, chromium coating of

high refractive index on the transparent disk surface in contact with the lubricant. Various improvements were proposed afterwards making possible to achieve extremely high levels of both sensitivity and resolution (spatial and temporal). This is certainly for these reasons that the interferometric methods are more than ever used today in EHL, and are still being developed further. The next sections give an overview of these evolutions.

Spacer layer. Despite the improvement offered by the employment of the semi-reflecting coating, film thickness measurement using conventional optical interferometry, both with monochromatic or chromatic illumination, suffered from some other limitations. These limitations rendered the measurements inaccurate to study very thin and/or relatively thick films, and the sensitivity became no more satisfactory.

The first limitation was imposed by interference rules, namely the necessity of having an OPD at least equal to half the wavelength of light, for such an interference to occur. Film thickness measurement is then limited to 50 nm at best (see Table 3). The second limitation is related to the color contrast decrease with increasing interference order, because of the fast decrease of reflected light intensity away from the center of the contact, and because the EHD contact forms an optical system that is not so perfect; beyond the sixth-eighth order, pastel shades prevail and colors become no more discernible. This prevented the mapping of wide-range film thickness variations. The third limitation is due to the fact that colors were identified by eyes and then compared to Newton's color scale for example, and eyes capabilities to distinguish colors limit film thickness measurement resolution to about 20 nm, in the best cases.

The first of these limitations was overcome after the work of Westlatke and Cameron[43] in 1967–1968, who proposed the deposition on top of the semi-reflective chromium coating of the so-called "spacer-layer", a thin transparent silica layer. Thanks to its refractive index very close to that of the oil, it permits the formation of interference fringes even in the absence of a lubricant oil. By subtracting the known thickness of the spacer layer from the total measured thickness (of the lubricant and the spacer layer thickness altogether), one can shift the lower limit of conventional optical interferometry down to very small values (10 nm typically).

Further developments permitted to shift even more this lower limit, and also to overcome the other two limitations. These developments became possible thanks to the large growth of technological capacity to store information and the availability of fast image capture equipment and image analysis methods. They permitted the emergence of three competing techniques (i) ultra-thin film interferometry (UTI), (ii) techniques based on image analysis and (iii) techniques based on fringes count.

Ultra-thin film interferometry. The principle was firstly developed by Israelachvili[44] in 1973 for its application in surface force apparatus (SFA). It is based on multiple-beam interferometry in which fringes of equal chromatic order (FECO) are analyzed. The author used a spectrometer for a more precise and objective analysis of the interferograms, rather than by simple eyes identification. These interferograms were obtained by transmission through thin films trapped between two transparent deformable sheets, and then read on a spectrogram. Using this system and a dedicated optical model, the author was capable to study thicknesses ranging between zero and few hundreds of angstroms, with a thickness resolution of 1 Å, and also to measure the refractive index of the fluid under investigation.

Whilst Israelachvili had developed this technique for SFA, Spikes et al.[45] extended and later applied it to film thickness measurements in the ball-on-disk test-rig configuration. They used the UTI term for the combination of a spacer layer with spectrometric analysis of the reflected light from a single location in the contact. This technique has been, and is still being used, in very different applications such as, for instance, the study of base oils[46] or polymer solutions[47] at high confinement. More recently, the UTI method was further refined[48] to allow film thickness measurements down to 0.3 nm, with a standard deviation of 0.15 nm. The detailed description of these works would be beyond the scope of this survey on *in situ* techniques in EHL; interested readers can refer to reviews on the subject, such as the one from Spikes.[7]

Image analysis. The alternative technique, based on image analysis techniques, was first developed by Gustafsson[49] in 1994. The availability of high resolution 3CCD detectors, low-cost frame grabbers, and image analysis softwares enabled (i) the problem of biased and insufficiently sensitive eyes reading to be overcome, and (ii) considerably more information (than naked eyes) about film thickness to be achieved in an automated way. This technique has the additional advantage of being much easier for full film thickness mapping than UTI which is generally applied to measure film thickness at individual locations. In this approach, colored interferograms are digitalized, and each pixel intensity and color information are converted into film thickness value at the corresponding point, via some calibrations obtained with known geometric shapes in static or steady-state conditions.

Gustafsson et al.[49] showed that this image processing method could be applied for ranges of film thickness between 90 and 700 nm. This approach was later applied in conjunction with spacer layers to measure film thicknesses down to 10 nm by Cann et al.,[50] who called this technique spacer layer imaging method (SLIM). A similar methodology was proposed by

Hartl et al.[51] called differential colorimetric interferometry (DCI), but based on a different calibration procedure and a different color space representation. They directly used the RGB signals (Red Green Blue) delivered by the camera against (Hue Saturation Intensity, or Lab) color transformation in previous works. Film thicknesses were measured between 5 and 800 nm, with a resolution of about 1 nm, and a spatial resolution close to 1 μm.

The works based on the advanced interferometric techniques described above proved the existence and validity of the EHL regime down to very low film thicknesses, of the order of a few tens of molecular dimension,[45,48,51] under very specific operating conditions: perfectly smooth surfaces, pure lubricants, inert relatively to the other used materials. They turned out also appropriate to establish the conditions under which the behavior of the lubricant was not predicted anymore by the classical EHD models. For instance, based on these methodologies, Dalmaz et al.[52] have improved and extended some EHD minimum film thickness expressions, a crucial point for estimating the actual lubrication regime.

Methods based on fringes count. The third technique, based on fringes count, was initially presented by Luo et al.[53] in 1996, and further refined by Guo and Wong.[54] Luo proposed an alternative approach, called relative optical interference intensity (ROII), to measure film thicknesses less than a quarter wavelength without requiring a spacer layer. In this approach, intensity variation of the reflected monochromatic beam is used, and the author reported a spatial resolution of $0.5 \times 1.5\,\mu m^2$, a film thickness measurement resolution of 0.5 nm, and a minimal detectable film thickness of less than 1 nm.

In Luo's approach, two-beam interference approximation was used. In 2002, Guo and Wong[54] improved the accuracy of this technique by carrying out a theoretical analysis taking into account the occurrence of multiple reflections within the film in addition to the absorptive nature of the metallic bounding surfaces (see Figure 10).

Infrared techniques

Generally speaking, Infrared (IR) radiation is used to investigate *in situ* physical and chemical phenomena thanks to the rich information that it contains. Through a careful analysis of the IR radiation emanating from the system under investigation or interacting with it, physical parameters (such as film thickness, temperature and pressure) can be measured, and chemical data (such as the actual chemical composition, chemical bonding of molecules, molecular orientation and alignment, and the tribochemical reactions) can be deduced.

IR spectroscopy or IR thermography? IR radiations can be studied both spectroscopically (IR absorption or emission spectroscopy), or simply by counting the total number of photons emitted from the material (IR thermography). Clearly, spectroscopic methods yield much more information than thermography. Each spectrum reflects indeed all the vibrational energy states within the material under investigation and their sensitivity to chemical or physical conditions, and they can thus be used to quantify or qualify these chemical bonds and the different parameters that have some of influence on them. Thermography can be used on the other hand, to measure the total IR emission which represents the total amount of vibrational energy in the material, or equivalently its temperature.

Both kinds of analysis have been used to investigate EHD contacts. However, even though IR spectroscopy provides physical information such as temperature, pressure and film thickness, it had less success than optical interferometry, Raman spectroscopy, and IR thermography. Indeed, it is a much complex technique with a limited spatial resolution.

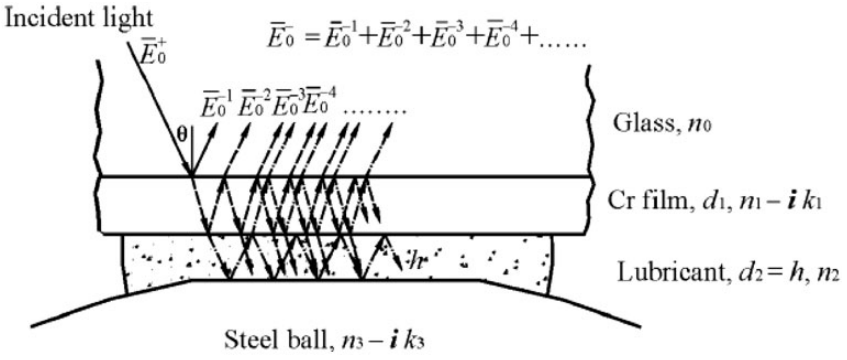

Figure 10. Model taking into account the multiple reflections and the absorptive nature of the bounding surfaces, from Guo and Wong.[54] Reproduced with the permission of the Institution of Mechanical Engineers and SAGE Publications Ltd.

IR spectroscopy. IR spectroscopy was initially developed in EHL by Lauer and Peterkin[55] in 1975. First experiments were conducted under static conditions in a high-pressure diamond cell. In a subsequent study,[56] they applied the method to a sliding EHD contact formed between a steel ball rotated over a small diamond disk. They showed that emission from the fluid and the ball surface could be separated in order to measure their respective temperature after some appropriate calibrations. Information such as phase and structural changes, viscosity and temperature could be deduced.

In 1991, Cann and Spikes[57] applied Fourier transform infrared (FTIR) spectroscopy to study lubricant films in and around an EHD contact formed between a steel ball rotating against a stationary disk transparent to IR radiation (diamond or CaF_2). An IR radiation, emitted by a conventional IR microscope, was focused within the contact, and its reflection at the lubricant/steel ball surface interface was collected with the same camera for a subsequent signal analysis. Film thickness is related to the amount of the reflection absorbed by the lubricant film, and pressure distribution is deduced from the spectrum bands shifts. For both measurements, some preliminary calibrations are necessary. Because of the limited spatial resolution of 100 μm, film thickness and pressure profiles were not sufficiently resolved (Figure 11).

IR thermography. The first application of IR thermography to study EHL was carried out by Winer and coworkers in the 1970s. The authors presented a series of papers in which they successfully applied this technique to map the temperature over the contact. In 1974, Turchina et al.[58] studied a sliding EHD point contact formed between a rotating steel ball loaded against a sapphire flat. They used an IR radiometric detector allowing the measurement, with a spot size resolution of 35.6 μm, of the ball surface and the lubricant film temperature rises within the contact. An analytical approach, combined with the use of an appropriate filter and some suitable calibrations, was applied to separate the four sources of radiations composing the total thermal emission, namely, the background, sapphire, steel ball and lubricant film emissions. The approach was slightly refined in 1976 by Ausherman et al.[59] who used a narrow and a wide band filters.

Temperature mapping was further developed in 2004 by Spikes et al.[60] who studied a rolling-sliding contact formed between a steel ball and a sapphire disk. Using a custom-built IR camera with an InSb detector, the authors were able to improve the resolution and to read temperature over approximately 11 μm non-overlapping spots. They applied different coatings to the disk—made from chromium and aluminum (see Figure 12(a))—in order to measure the temperature on both contacting surfaces. They could perform these measurements by considering that:

– Some small proportion of the IR radiation is emitted from the lubricant, but it can be removed with a long wave filter.

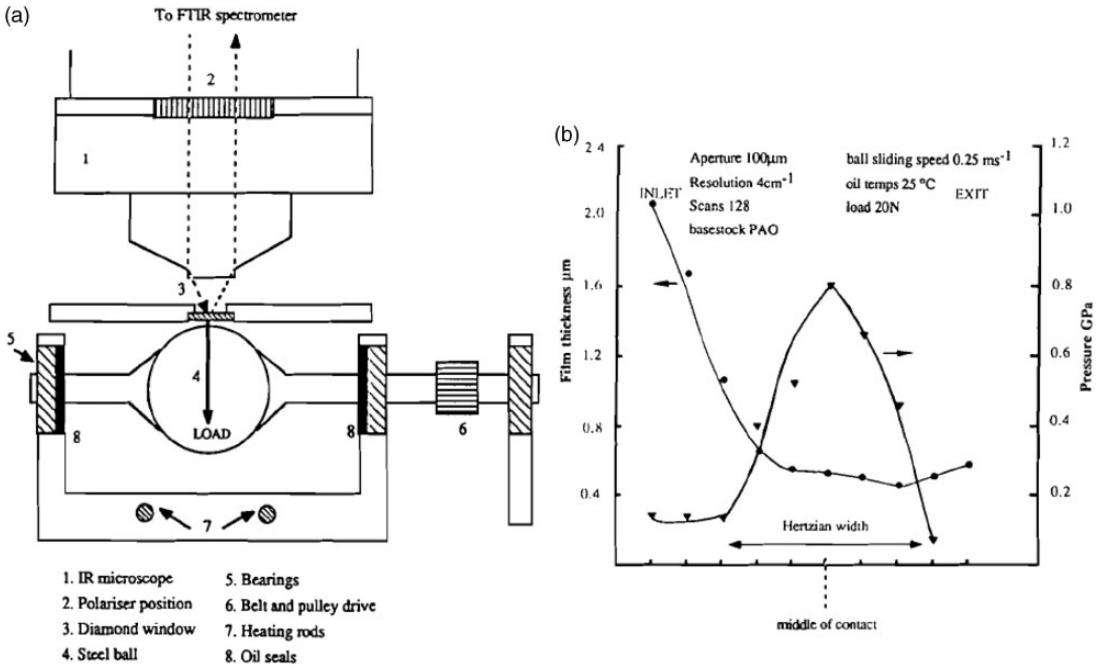

Figure 11. (a) A schematic of the arrangement used for temperature measurement by IR spectroscopy; (b) film thickness and pressure profiles obtained in an EHD sliding contact from IR spectroscopy. Reproduced with permission of Taylor & Francis from Cann and Spikes.[57]

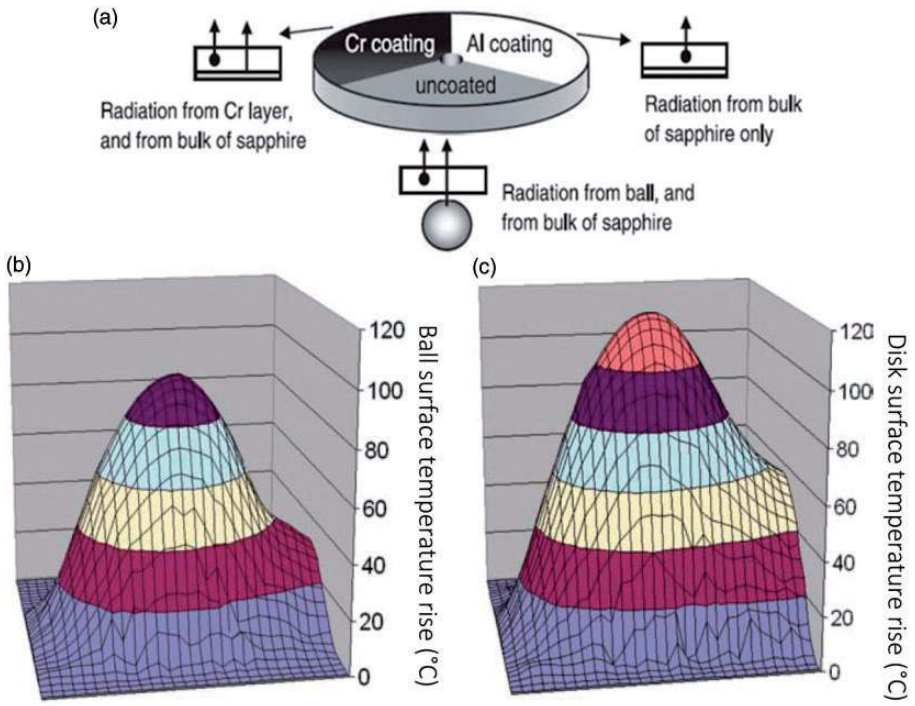

Figure 12. (a) Different coatings used by Spikes et al.[62] to map temperature by IR thermography. Reproduced with the permission of the Institution of Mechanical Engineers and SAGE Publications Ltd. (b) and (c) Typical temperature rises obtained by IR thermography. Reproduced with kind permission of Springer Science and Business Media from Spikes et al.[60]

- Most of the emission passing through the uncoated sector originates essentially from the steel ball surface and from bulk sapphire.
- Chromium is a fully reflective material to IR radiation, thus when the chromium-coated sector passes through the contact, the detected emission emanates from the chromium layer (or the sapphire disk surface) and also from bulk sapphire.
- Aluminum is a poor emitter material, and allows the radiation from the bulk sapphire to be detected.

The emission emanating through the uncoated and the chromium sectors can yield the temperature of the surface of the steel ball and the bottom surface of the sapphire disk, respectively. But prior to that, these emissions have to be corrected by removing the sapphire hot body emission, detected from the aluminum-coated sector.

Temperature maps were obtained using this method with a spatial resolution of 11 μm and for various sliding conditions. Figure 12 shows some examples of temperature rises over the ball (Figure 12(b)) and the disk (Figure 12(c)) surfaces at a slide-to-roll ratio of 100 % (ball moving faster). From these data used as boundary conditions, the authors derived shear stress maps and local friction coefficients within the contact, using moving heat source theory.

In 2005 Yagi et al.[61] conducted IR emission measurements with a better sensitivity with the aim to clarify the mechanisms of dimple formation under sliding conditions in EHL. For this purpose, a contact was formed in steel-ball / sapphire-disk device equipped with a new generation of IR camera. Depending on the employment of uncoated or chromium-coated disk, the ball surface temperature or the disk surface temperature were measured, respectively. Temperature profiles were estimated by assuming a parabolic variation through the oil film and, more remarkably, temperature distribution through film thickness were obtained. Some examples are shown in Figure 13.

In 2009, Reddyhoff et al.[62] improved the sensitivity and spatial radiation (compared to the one obtained by using stepping microscope techniques) to 6 μm, and this by employing a high specification full-field IR camera and a custom-built microscope lens. A rectangular area of 2.0 × 1.61 mm was covered in each temperature map. By inspiring from Spikes work[57] (see Figure 12(a)), a similar approach was applied in order to separate the different components of the IR emission. In order to remove any compression heating or cooling and, in this way, isolate temperature heating arising from shearing, the authors subtracted temperature rise maps obtained under pure rolling conditions from sliding temperature maps. According to the authors, this approach removes in the same time some optical aberrations. With these new facilities, Reddyhoff et al.[62] were able to achieve temperature profiles under more

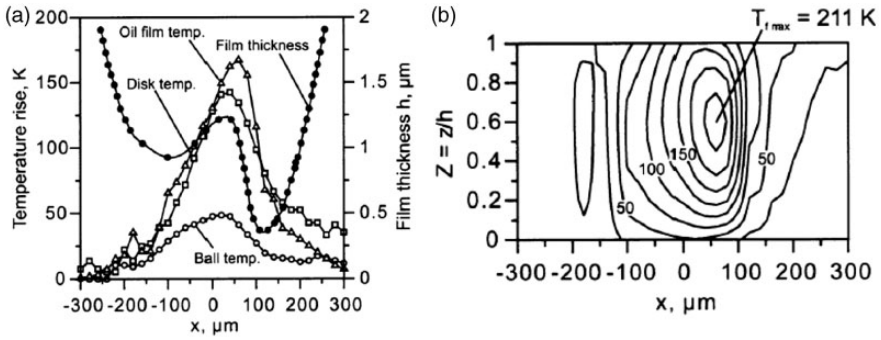

Figure 13. Temperature rise and film thickness (measured via duochromatic interferometry) profiles in dimple zone (a.) through-thickness temperature map (b.) Published by ASME, Figure 10(b) from Yagi et al.[61]

representative conditions of pressure, slide-to-roll ratio, nature of the lubricant than those Spikes et al.[57] imposed 5 years before.

Raman spectroscopy

A brief description of the physical origin of Raman diffusion is first proposed. The illumination of a sample with a monochromatic light is followed by different processes. While almost all the light is reflected or transmitted without any light-matter interaction, a small fraction of the absorbed light is re-emitted in all directions without any change in frequency. This process is thus an elastic light diffusion and is called Rayleigh scattering. An even weaker fraction of light is scattered with some energy change, and this change is due to some variation of excitation energy within the sample molecules, in the form of vibrational energy. This light diffusion is therefore inelastic, and is called Raman scattering. These energy changes can be either positive or negative, in which the case the diffusion is termed Stokes or anti-Stokes, respectively. The Stokes and anti-Stokes diffusion peaks are located symmetrically around the Rayleigh peak. This symmetry is due to the transition in opposite directions between the same upper and lower vibrational energy states in the Stokes and anti-Stokes shifts. In contrast, their intensities are different, as they depend on the population of the different energy states prior to excitation. Following thermodynamic equilibrium, an upper state is less populated than a lower one, which results in a higher rate of Stokes transitions (towards the upper states) compared to the rate of anti-Stokes transitions (towards the lower states). A more detailed description of the Raman effect can be found in the literature, e.g. in the two books by Long[63] and Ferraro et al.[64]

From this description, Raman spectrum is directly related to the vibrational energy of the sample, and is consequently characteristic of the material under investigation. It can yield qualitative or quantitative information about its chemical structure and bonds. Furthermore, the influence of some physical parameters can extend to the molecular scale of the matter and this allows Raman spectroscopy to be used to measure them. In what follows, only the measurement of film thickness, pressure and temperature via Raman spectroscopy will be considered, as it is directly related to the aim of this review. Each parameter can be theoretically determined by an independent procedure:

- The intensity of the Raman peaks is proportional to the number of shone molecules, which itself is proportional to film thickness. This allows film thickness to be measured after an appropriate calibration.
- The application of an external pressure reduces the equilibrium inter-atomic distances, which induces some changes in vibrational energy within the molecules and results in the shift of the corresponding Raman peaks. The knowledge of the energy shift dependence on pressure allows for pressure measurements in pressurized lubricated contacts, as those found in EHL.
- The relative population between an upper and a lower energy state depends on temperature, which implies the dependence of the relative intensity of Stokes and anti-Stokes peaks on this parameter, and permits the temperature to be measured.

The application of Raman spectroscopy in tribology has been pioneered by Gardiner et al. in 1980s. They first employed it to measure the pressure in a static entrapment between a ball and a flat.[65] In another study, the authors applied it to a realistic EHD contact formed between a rolling ball and a flat.[66] In both studies, as well as the most of those presented in this section, the polyphenyl ether fluid 5P4E was used as lubricant, for different reasons:

- A highly Raman scattering material is required because of the intrinsic weakness of Raman signal and, for the same reason, this material should be capable to form a relatively thick film under EHD conditions.

– At the same time, using an intense light source to produce a stronger Raman signal is not an appreciated alternative as it can induce undesirable heating and even the collapse of the lubricant film.
– Many lubricants, and particularly mineral oils, are not suitable since they have a strong fluorescence signal capable of hiding the Raman bands.

The use of Raman spectroscopy to probe film thickness in EHD contacts encountered actually no marked success, on the one hand because it requires the same constraints as interferometry (presence of a transparent material) but the latter is much simpler to implement, faster and fully validated. On the other hand, Raman spectroscopy presents in the best case an extremely low signal-to-noise ratio: combined with film thicknesses of a few hundred nm, the intensity measurement and its quantitative calibration become tedious and again, the interferometric techniques are by far more efficient. When it comes with the temperature measurement, it turns out that this method does not yield sufficient measurement sensitivity regarding temperature rises expected to occur in EHD contacts. As an illustration, in the best case a temperature resolution between 5°C and 20°C was theoretically predicted by LaPlant et al.[67]

Despite these limitations, Raman technique offers a clear advantage in terms of spatial resolution against IR spectroscopy. Gardiner et al.[66] obtained pressure distributions in agreement with theoretical predictions and they could, in particular, observe qualitatively the Petrusevich pressure spike located at the exit of the contacts. In 1995, Hutchinson et al.[68] used Raman spectroscopy to measure film thickness around a static contact formed between a steel ball and a diamond window. After establishing a relation between film thickness and Stokes peak intensity, the authors measured film thicknesses ranging from 0.1 to 10 µm, with a spatial resolution of 7 µm.

Jubault et al.[69] published several studies in which pressure mapping was achieved by coupling an EHD tribometer with a high-resolution Raman spectrometer. They showed that under specific conditions, an EHD contact in pure rolling can be considered as a high-pressure cell: the frequency shift dependence on pressure of another fluid (a 8CB liquid crystal) was calibrated up to 1.4 GPa from *in situ* test performed with a ball-on-disk tribometer. Pressure measurement sensitivity and spatial resolution were then improved to reach around 30 MPa and 10 µm, respectively.[70] They obtained pressure profiles and maps in which Petrusevich pressure spike and its variations with load and speed were clearly evidenced (Figure 14). In further works, the authors obtained pressure profiles under various normal load and rolling-sliding conditions.[71] They also succeeded in carrying out measurements of pressure distributions within artificially dented contacts[72] or in the presence of the so-called dimple phenomena.[73]

Fluorescence methods

Photoluminescence (PL) is light emission by a molecule (or by any form of matter) after being electronically excited with photons. Figure 15 shows a

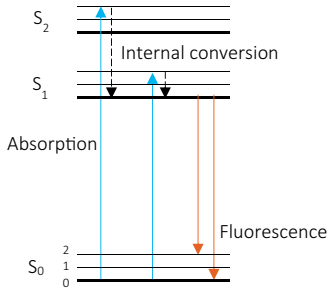

Figure 15. A simplified Jablonski diagram.

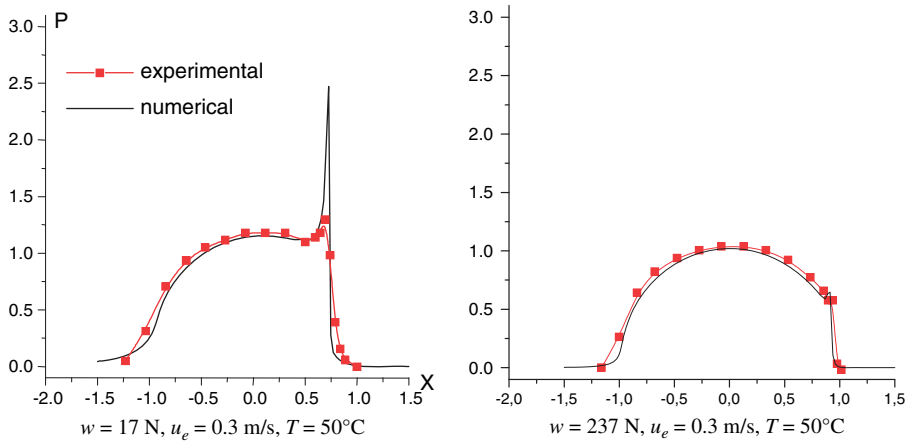

Figure 14. Pressure profiles (dimensionless variables) obtained by Raman microspectrometry, compared with numerical solutions. Reproduced with permission of Elsevier from Jubault et al.[70]

simplified form of Jablonski diagram[74] that can be used to illustrate the different forms of PL. In this diagram, the energy levels are schematically depicted as horizontal lines. The thicker lines are representations of the limits of electronic energy states (S_0, S_1, S_2) whereas the thinner lines represent the multiple vibrational states associated to each electronic state.

Following light absorption, an electron of the molecule is excited from ground state S_0 to one of the excited vibrational levels of the first or the second electronic levels, S_1 and S_2. The relaxation of this electron to its ground state is accompanied by energy dissipation following different mechanisms. One of these mechanisms is the emission of a photon: fluorescence. It is worthy to note that the energy of fluorescence photons is generally less than that of the exciting ones. This property, called Stokes shift, takes place due to the amount of energy generally lost through internal conversion before fluorescence emission. It is a valuable feature for spectroscopic studies: it allows the separation of the excitation background from emission band without reducing the sensitivity of fluorescence-based techniques.

Film thickness measurement. Smart and Ford[75] were the first to apply fluorescence in tribology in 1974. The aim of their work was to measure free lubricant film thickness on roller and raceway surfaces. UV mercury-vapor lamp wavelength of about 365 nm was used to shine the contact (see Figure 16(a)). The natural intensity of the fluorescence of the oil, or the fluorescence of suitable particles dispersed in the oil, emitted in the range of visible light and proportional to the number of fluorescence molecules was then measured to deduce film thickness (see Figure 16(b)). Later in 1978, Ford and Foord[76] improved the previous arrangement by replacing the mercury lamp with a He–Cd laser simplifying the associated optics and increasing the working distance. They also compared UV excitation and visible blue excitation, and found that the latter can be a promising alternative. These works were the initiation of the so-called LIF, or laser-induced fluorescence technique, in which the fluorescent specie is excited with a laser at some wavelength and the emission at another wavelength is detected due to the Stokes shift property of fluorescence emission. Film thickness is then measured after separating emission from excitation by using some filters (see Figure 16).

The use of a CCD video camera (instead of a photomultiplier) with a personal-computer-based signal analyzer permitted to measure,[77] in a single-cylinder research engine, the oil film thickness distribution around the piston under various operating conditions.[78] The results indicated that oil film was thinner near the edges of the bearing than at the center in all tested conditions. However, these works, dedicated to automotive applications, were successful in measuring film thickness but only for higher ranges (typically from 0.5 up to a few tens of micrometers) than those of interest in EHL. The works of Sugimura et al.[79] clearly confirmed the limitation of fluorescence to large film thicknesses, especially because of the presence of internal interferences. This drawback can, however, be transformed into an opportunity for studying high-thickness and soft-EHD contacts in which one counterface can be made from polymer, elastomer or from any material found in natural joints for instance.

Flow measurement. Fluorescence imaging has also been applied in the measurement of fluid flow within lubricated contacts. Different techniques exist, the simplest consist of:

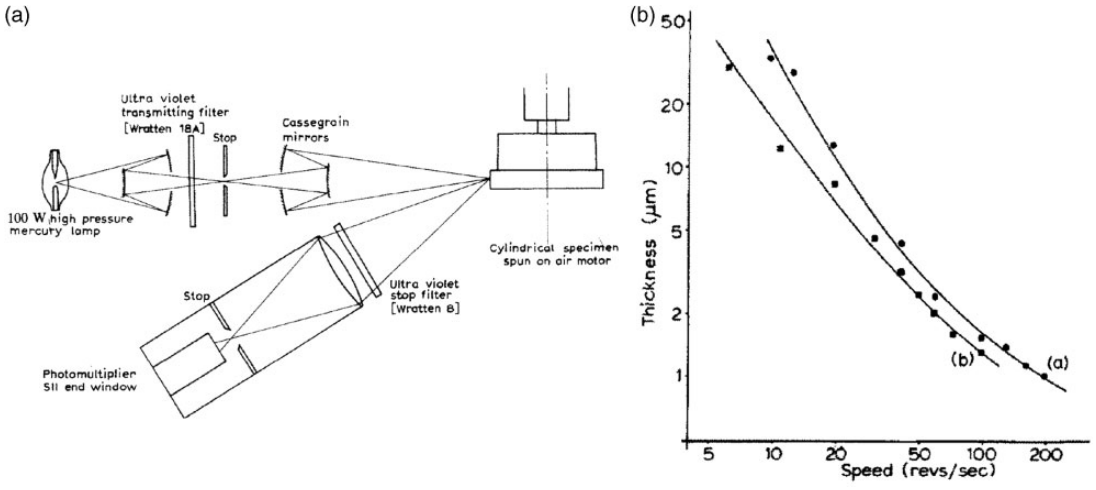

Figure 16. (a) Optical arrangement in the earliest development of film thickness measurement by fluorescence; (b) film thickness vs. speed. Reproduced with permission of Elsevier from Smart and Ford.[75]

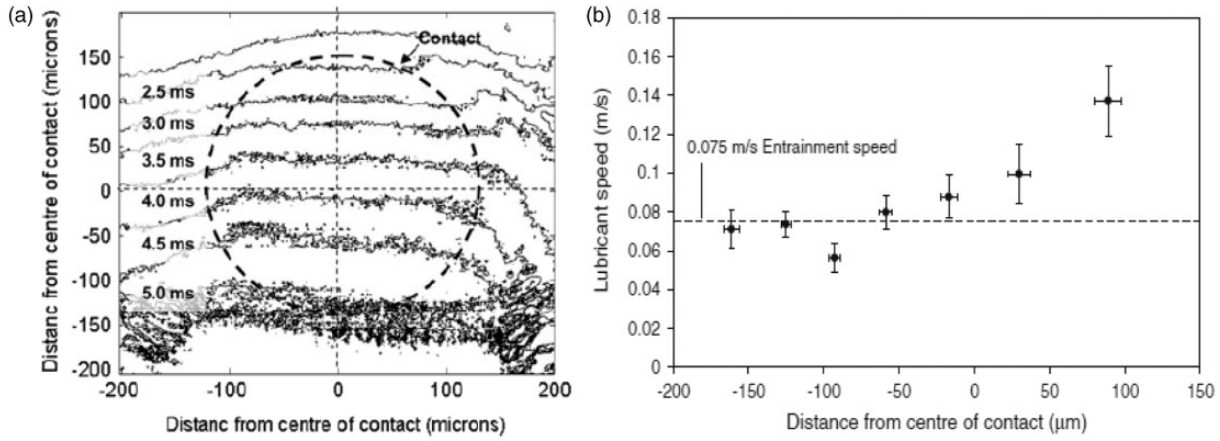

Figure 17. (a) Dye progression from the inlet (top) to the outlet (bottom) of the contact, and (b) lubricant speed along the contact. Reproduced with kind permission of Springer Science and Business Media from Reddyhoff et al.[80]

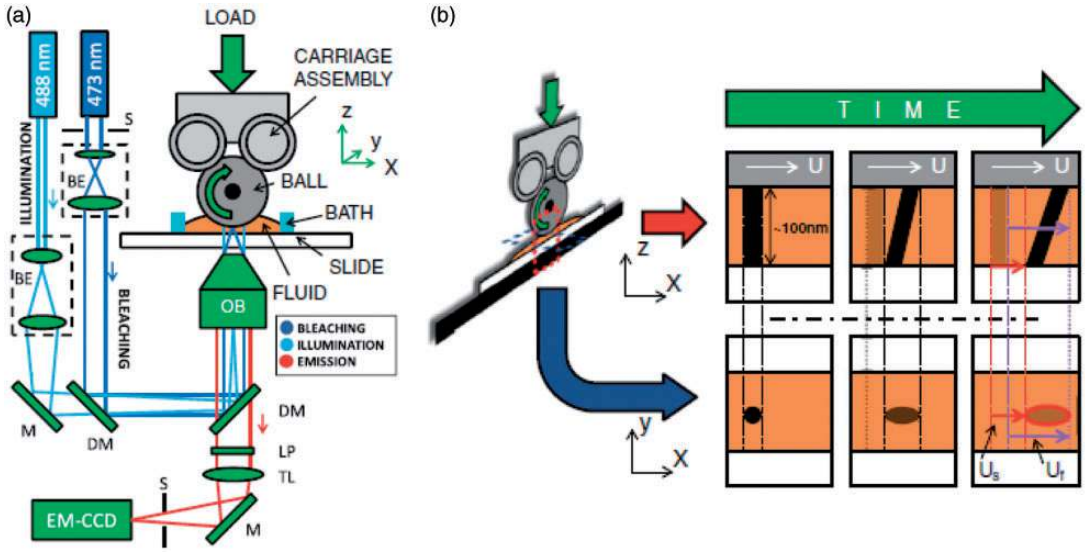

Figure 18. (a) Schematic of the FRAP arrangement; (b) position and shape of the photobleached plug as observed in the *x*,*y*-plane and derived in the *x*,*z*-plane. Reproduced with kind permission of Springer Science and Business Media from Ponjavic et al.[81]

– Flooding the contact with doped or undoped lubricant and, in the latter case, fluorescent dyes are added on demand at the inlet of the contact,
– Monitoring the motion of the doped lubricant as it crosses the contact zone.

An application of this technique was conducted by Reddyhoff et al.[80] who studied the lubricant flow in a rolling contact formed between a steel ball and a glass disk. In this study, the advancing forehead of a droplet, containing Eosin dye (at a concentration of 0.04 wt%) previously deposited upstream the contact, was recorded over time. A pulsed laser with a wavelength of 532 nm and a high-speed intensified camera were used. The dye progression through the lubricated ball-on-disk contact (Figure 17(a)) was monitored, and an increasing mean speed along the contact main direction was derived (Figure 17(b)).

Another study of interest for EHL has been conducted in 2014 by Ponjavic et al.[81] aiming to measure through-thickness velocity profiles by inspiring from optical techniques devised by Leger et al.[82] and called fluorescence recovery after photobleaching (FRAP). This *in situ* methodology includes the following steps:

– Dissolve a fluorescent dye in the lubricant.
– Focus an intense blue laser of a wavelength of 473 nm in order to bleach a small column, called photobleached plug, within the lubricant.
– Excite the lubricant by a low intensity cyan laser of 488 nm.

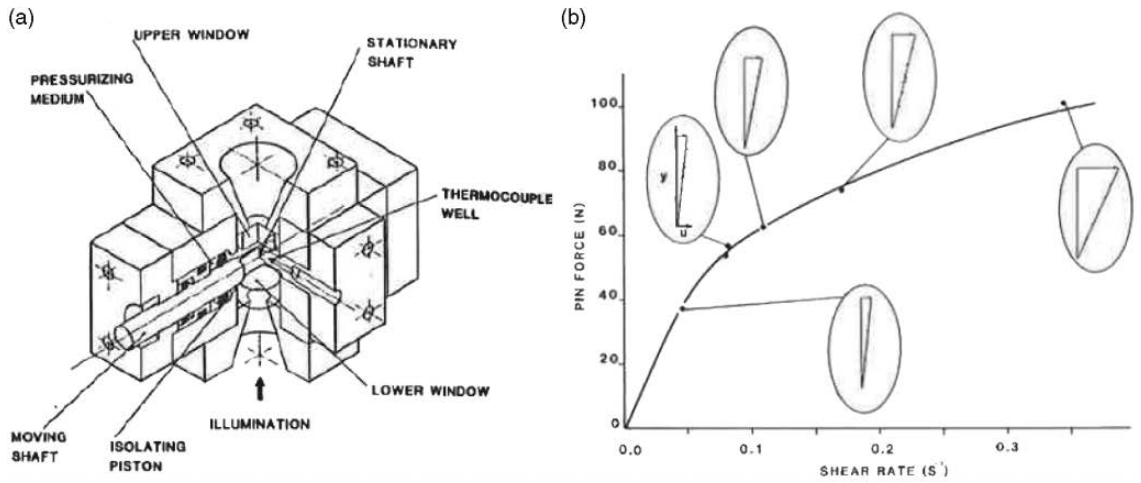

Figure 19. (a) High-pressure visualization flow visualization cell; (b) typical set of velocity profiles obtained under different conditions in 5P4E. Published by ASME, Figures 3 and 6 from Bair et al.[83]

– Map the fluorescent intensity of the lubricant to observe the motion and the shape of the photobleached plug, eventually determine the velocity profile after some mathematical and physical considerations (see Figure 18(a) and (b)).

This approach has been validated in a simulated Couette flow in which a linear velocity profile was expected, and applied to an EHL contact where significant deviation was observed.

Advantages and disadvantages. To end our brief description on the application of fluorescence technique for *in situ* measurements, we can point out some of its advantages and disadvantages.

The main advantage is that it does not require reflective coating of the contacting surfaces. These coatings are liable to wear, particularly when the contact is formed between rough surfaces, and this allows film thickness to be monitored under these conditions. Also, a higher upper limit than optical interferometry to film thickness measurement is expected, since the fluorescence emission intensity can be controlled by the extent of lubricant doping, but this potential advantage does not really concern EHL.

The common disadvantage of optical methods is the necessity of employing at least one transparent surface, which is also true in the case of fluorescence imaging. The other limitation is related to the fact that the emission intensity is proportional to the amount of lubricant present in the gap between the two surfaces. This implies that under thin film EHL regime or in cavitation conditions film thickness cannot be quantitatively determined.

Particle image velocimetry

Another technique that can be classified among optical methods is particle image velocimetry. This technique is being progressively applied over the last decades in flow visualization in different scientific and technological contexts. It is based on illuminating sufficiently small particles doping the fluid under investigation to make instantaneous velocity measurements. These measurements assume that the local particle velocity is identical to the local carrying liquid velocity, or in other terms, the particles are supposed to faithfully follow the fluid flow. This condition has to be satisfied by a proper choice of tracers' properties.

PIV has been applied in 1993 by Bair et al.[83] to elucidate the mechanisms leading to the intriguing phenomena of limiting shear stress observed in concentrated lubricated contacts and which lacks solid theoretical foundations. A test cell has been designed for this purpose allowing the fluid to be sheared under high pressure and the local velocities to be visualized (see Figure 19(a)). A particle concentration of 0.1 wt% was used in all the tests, and different tracers were tested:

– Carbon black particles with 0.3 μm diameter.
– Polystyrene tracer spheres with fluorescent dye.
– Glass spheres of 2 μm diameter visible in the model lubricant 5P4E.

Velocity profiles were obtained by determining the ratio of particle displacement to the measurement time (which varied between one to two seconds). A set of velocity profiles are shown in Figure 19(b). Good correlation to wall velocities were obtained when the measured velocities were extrapolated in the proximity of the wall (extrapolation was needed since the liquid at 20 μm from the wall was obscured).

More recently, Horvat and Braun[84] performed flow measurements in hydrostatic journal bearings. A high intensity YAG laser, combined with a specific optical system, was used to create a thin planar sheet of light

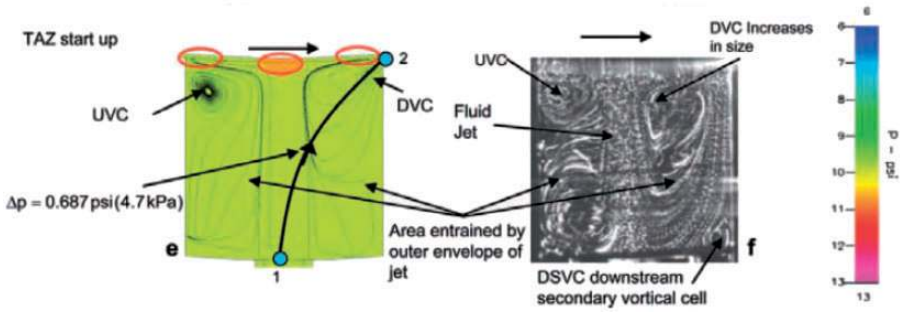

Figure 20. Example of flow patterns obtained numerically and experimentally in the pocket of a hydrostatic journal bearing. Reproduced with permission of Taylor & Francis from Horvat and Braun.[84]

in which the seed particles were tracked in a Lagrangian fashion, allowing in this way the instantaneous flow pattern to be constructed in any desired plane (see Figure 20 for an example of comparison between numerical and experimental flow patterns).

Alternative methods

Acoustic method

The application of acoustic method in film thickness measurement in tribological systems is still in its infancy as it dates back to the beginning of the 2000 s. It combines two main advantages: (i) it is a noninvasive method and (ii) it does not require a transparent material and can thus be applied to real machine components.

It was first applied by Dwyer-Joyce et al. in 2003[85] in different systems: fluid layers between flat plates, fluid layers between eccentric rings, an EHD lubricant sliding contact formed in a ball-on-flat device, and finally a rolling element bearing. An ultrasonic pulse-receiver (UPR) was used to generate a high-voltage pulse. A piezoelectric transducer in mechanical resonance is excited with this pulse and emits a broadband pulse of ultrasonic energy. This pulse is received by the same transducer after being reflected from the lubricant layer. The reflected pulse is amplified and finally modeled by a spring-model method or a continuum method to deduce film thickness value (see Figure 21(a)). The investigation of the two first systems proved the feasibility of the newly proposed approach (Figure 21(b)). Good agreement between measurements and theoretical predications was found in the two other systems working under EHL regime (Figure 21(c) and (d)). In the latter, the authors could record film thicknesses ranging between 50 and 500 nm. A lower limit of about 2 nm was estimated for these measurements and the authors expected that there is no upper limit (see Figure 21(b)).

In another paper[86] presenting the operating limits of film thickness measurement via acoustic method, Dwyer-Joyce et al. used the following formula to estimate the spatial resolution obtained by a focused transducer

$$d_{f(-6dB)} = \frac{1.028Fc}{fD} \tag{2}$$

where d_f is the diameter of the spot size (the signal being reduced to -6 dB of its peak value), F the transducer focal length, c the speed of sound in the focusing medium, f the wave frequency, and D the diameter of the piezo element.

Figure 22, plotted for a typical transducer, shows the value of the frequency that has to be selected to get the desired spot size. A minimal physical value to the spatial resolution is dictated by the wavelength ($\lambda = c/f$) of the ultrasonic pulse. In the frequency range between 10 and 50 MHz of an ultrasonic pulse moving in steel, this minimal value is between 590 and 118 μm, respectively. It is clear that this spatial resolution can only provide an averaged value of film thickness, and this is the major drawback of the acoustic approach.

Other possible in situ *techniques*

There are many techniques that have been reported in the literature allowing for the measurement of all the above-mentioned parameters in other scientific and technological contexts such as in biology, microelectronics and microfluidics. The principle of some of these methods is briefly recalled in Table 4 with some metrological features, namely their resolutions.

The possibility of implementing any of these techniques (or others) in EHL can be examined by considering some general criteria, in particular:

- The accessibility of the interface has to be ensured.
- The technique's inevitable interference with *in situ* conditions has to be negligible or corrigible.
- The sensitivity of the technique to the investigated parameter should be sufficiently large for the

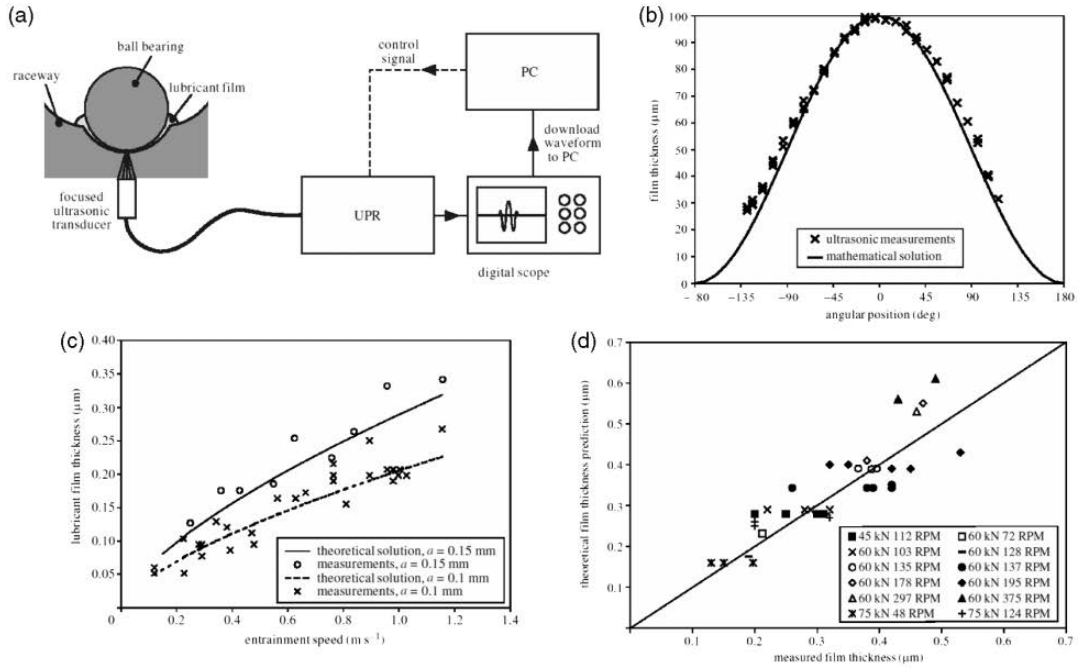

Figure 21. (a) Schematic of the acoustic measuring device. Comparison between the measured and the theoretical film-thickness value in (b) an annular oil-film apparatus, (c) a ball on disc EHL apparatus (d) a rolling bearing. Reproduced with permission of the Royal Society from Dwyer-Joyce et al.[85]

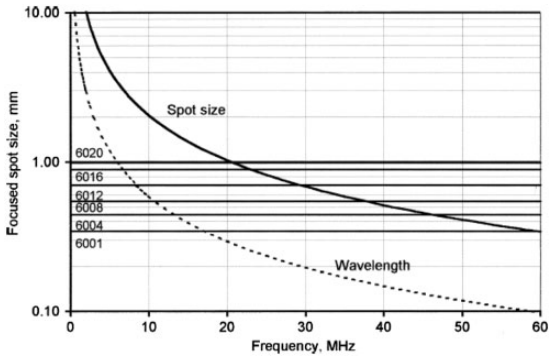

Figure 22. Spot size dependence on frequency (for a transducer of spherical focal length of 25 mm and a diameter of 7.5 mm). Reproduced with permission of Taylor & Francis from Dwyer-Joyce et al.[86]

detection of the variations occurring to this parameter under EHD conditions.

- Measurement timescale offered by the technique should be much shorter than characteristic times encountered in EHL.
- Besides the sensitivity to the investigated parameter has to be unaffected to the other (external or internal) parameters, or at least, any deviation induced by undesired sensitivities has to be corrigible or measurable.
- The technique should be unaffected by the extreme conditions occurring in EHL, or at least, sufficiently resistant allowing measurements to be carried out properly within the time required for these measurements.

Depending on the measurement requirements for a given application, metrological features can determine whether or not a technique is suitable, or can help favoring a technique over another, for example:

- The spatial resolution,
- The sensitivity to the investigated parameter,
- The minimal and the maximal measureable values,
- The timescale of the measurement if transient effects can occur.

To give some examples, high spatial resolution is required if a careful mapping has to be carried out, or if some sharp variation (such as the Petrusevich pressure spike) has to be observed. Slight temperature variations due to compression need obviously very sensitive measurements. The minimal measurable film thickness is of crucial importance in the selection of an adapted illumination for interferometric methods (monochromatic, duochromatic, or chromatic). And finally, the study of the influence of vibrational effects occurring in some mechanical components requires sufficiently small response times.

Although some of the methods presented in Table 4 yield interesting measurement features, their applicability in tribological context is out of the scope of this document and will not be discussed in detail. However, in order to illustrate the importance of the above-mentioned general criteria some examples can

Table 4. Overview of new potential *in situ* techniques for investigating EHD contacts.

Measured parameter	Technique	Principle	Measurement resolution	Spatial resolution
Temperature	Microthermocouples	Temperature dependent voltage difference	0.01 K	$\geqslant 15\,\mu m$[91]
	Scanning thermal microscopy (SThM)	Temperature sensitivity of a thermocouple or a resistive probe fixed on the tip of an atomic force microscope (AFM) cantilever	0.1 K[92]	50 nm[92]
	Near-field scanning optical microscopy (NSOM)	Sample surface temperature-dependent reflectivity measured through the evanescent waves emitted by the surface after being illuminated by a tip	1 K	20 nm
	Fluorescent micro-thermography (FMT)	Quantum efficiency of fluorescent molecules or particles	0.001 K[93]	0.3 μm[93]
	Thermoreflectance	Refractive-index thermal dependence	0.01 K[94,95]	0.3 μm[94,95]
	Liquid crystal thermography (LCT)	Temperature-induced phase transition	About 0.1 K[96]	2–4 μm[96]
Pressure	Fluorescence spectrometry	Semiconductor nanoparticles Fluorescence wavelength shift due to pressure effects[97]	To explore	To explore
Flow	Nanoparticle image velocimetry	Tracking fluorescent nanoparticles dispersed in the fluid under investigation	To explore	50 nm (through thickness)[81]
	Atomic force microscopy	Torsional twist dependence on velocity of a 50 nm diameter whisker immersed in the liquid film	To explore	50 nm

be given. All near-field techniques, i.e. those requiring an extremely close proximity between a sensor fixed on a tip and the sample (such as SThM and NSOM for temperature measurement, and atomic force microscopy for flow measurement) seem not suitable for *in situ* investigation of EHL because of accessibility restriction. As regards the feasibility of temperature measurement by using liquid crystal coating or temperature/pressure measurement by employing fluorescent particles or molecules, the resistance of these sensors to temperature, pressure, and sliding conditions typical of the EHL regime is probably one of the first issues to be considered. Finally with the current emergence of nanotechnologies[87–90] everywhere around us, it would not be surprising in the very near future that these techniques can be adapted for the *in situ* analysis of EHD contacts.

Conclusion and recommendations

Different relevant *in situ* methodologies for investigating EHD contacts have been described and some important results have been presented. It appeared from this review that the evolution of each of these techniques was guided by technological advances. To summarize on what can be considered as the most successful approaches, we can conclude that optical interferometry, IR thermography, and Raman spectroscopy are techniques that have enabled, with high levels of resolution and sensitivity, to map film thickness, temperature, and pressure, respectively. Among these parameters, film thickness and temperature were the most studied.

Unfortunately, these performing methodologies provided a single information only. In other words, no technique was found allowing for *in situ* quantitative temperature and pressure, or thickness and temperature, or pressure and thickness measurement in EHL through a single experimental bench.

Other techniques exist that can be exploited, especially for temperature and pressure measurement. The effort in developing new or more efficient or accurate *in situ* methodologies must be pursued. Beyond assisting in the knowledge of the physical parameters acting at the micro- or nanoscale within the contact, they offer a unique opportunity for (i) improving the understanding of some unresolved questions (limiting shear stress, slip at wall, amplitude and transport of shear heating) and (ii) validating the numerical modeling not only at a single location but also on the whole contact area. From this, the complementarity between experimental techniques and numerical models is more than ever desirable.

Finally, there exists a further need in exploring EHD contact, mostly related to the above-mentioned unresolved questions. It concerns the mapping of not only the velocity field across film thickness as some groups currently try to achieve but the *in situ* measurement of the shear stress over the contact surfaces

and in between. But in the end, is the correct prediction of friction not the first concern (or the Graal) of any tribologist?

Conflict of interest

None declared.

Funding

The authors are indebted to the Carnot Institute Ingénierie@Lyon (I@L) for its support and the funding of the NanoFluo project.

References

1. Ertel MA. Hydrodynamic calculation of lubricated contact for curvilinear surfaces. In: *Proceedings of CNIITMASh*, 1945, pp.1–64.
2. Jablonka K, Glovnea R and Bongaerts J. Evaluation of EHD films by electrical capacitance. *J Phys D Appl Phys* 2012; 45: 385301.
3. Siripongse C, Rogers PR and Cameron A. Discharge through oil films. *Engineering* 1958; 186: 146–147.
4. MacConochie IO and Cameron A. The measurement of oil-film thickness in gear teeth. *J Fluids Eng* 1960; 82: 29–34.
5. Ibrahim M and Cameron A. *Oil film thickness and mechanisms of scuffing in gear teeth*. London: Institution of Mechanical Engineers, 1963, pp.228–238.
6. Dyson A. Investigation of the discharge-voltage method of measuring the thickness of oil films formed in a disc machine under conditions of elastohydrodynamic lubrication. *Proc Instn Mech Engrs* 1966; 181: 633–652.
7. Spikes HA. Thin films in elastohydrodynamic lubrication: The contribution of experiment. *Proc IMechE, Part J: J Engineering Tribology* 1999; 213: 335–352.
8. Glovnea R, Furtuna M, Nagata Y, et al. Electrical methods for the evaluation of lubrication in elastohydrodynamic contacts. *Tribol Online* 2012; 7: 46–53.
9. Lane TB and Hughes JR. A study of the oil-film formation in gears by electrical resistance measurements. *Br J Appl Phys* 1952; 3: 315–318.
10. Needs SJ. Boundary film investigations. *Trans Am Soc Mech Eng* 1940; 62: 331.
11. Furey MJ. Metallic contact and friction between sliding surfaces. *ASLE Trans* 1961; 4: 1–11.
12. Tallian TE, Chiu YP, Huttenlocher DF, et al. Lubricant films in rolling contact of rough surfaces. *ASLE Trans* 1964; 7: 109–129.
13. Palacios JM. Elastohydrodynamic films in mixed lubrication: An experimental investigation. *Wear* 1983; 89: 203–213.
14. Kannel JW, Bell JC and Allen CM. Methods for determining pressure distributions in lubricated rolling contact. *ASLE Trans* 1965; 8: 250–270.
15. Cheng HS and Orcutt FK. A correlation between the theoretical and experimental results on the elastohydrodynamic lubrication of rolling and sliding contacts. *Proc Instn Mech Engrs* 1965; 180: 158–168.
16. Orcutt FK. Experimental study of elastohydrodynamic lubrication. *ASLE Trans* 1965; 8: 381–396.
17. Hamilton GM and Moore SL. Deformation and pressure in an elastohydrodynamic contact. *Proc R Soc A Math Phys Eng Sci* 1971; 322: 313–330.
18. Safa MMA, Anderson JC and Leather JA. Transducers for pressure, temperature and oil film thickness measurement in bearings. *Sens Actuat* 1982; 3: 119–128.
19. Kannel JW and Dow TA. The relation between pressure and temperature in rolling–sliding EHD contact. *ASLE Trans* 1980; 23: 262–268.
20. Höhn B-R, Michaelis K and Kreil O. Influence of surface roughness on pressure distribution and film thickness in EHL-contacts. *Tribol Int* 2006; 39: 1719–1725.
21. Miyata S, Höhn B-R, Michaelis K, et al. Experimental investigation of temperature rise in elliptical EHL contacts. *Tribol Int* 2008; 41: 1074–1082.
22. Marginson HJ, Sayles RS and Olver AV. Limitations of thin film microtransducers in highly loaded contacts. *Tribol Int* 1995; 28: 517–521.
23. Wilczek A. Influence of electrical parameters of a thin-layer sensor on the accuracy of pressure measurement in an EHD contact. *J Tribol* 2011; 133: 31504.
24. Wilczek A. The influence of construction features of a thin-layer sensor on pressure distributions recorded in an elastohydrodynamic contact. *J Tribol* 2012; 134: 11501.
25. Crook AW. The lubrication of rollers. *Philos Trans R Soc A* 1958; 250: 387–409.
26. Crook AW. Elastohydrodynamic lubrication of rollers. *Nature* 1961; 190: 1182–1183.
27. Dowson D and Higginson GR. A numerical solution to the elasto-hydrodynamic problem. *J Mech Eng Sci* 1959; 1: 6–15.
28. Archard GD, Gair FC and Hirst W. The elasto-hydrodynamic lubrication of rollers. *Proc R Soc Lond A* 1961; 262: 51–72.
29. Dyson A, Naylor H and Wilson AR. The measurement of oil-film thickness in elastohydrodynamic contacts. *Proc Instn Mech Engrs* 1965; 180: 119–134.
30. Hamilton GM and Moore SL. Measurement of the oil-film thickness between the piston rings and liner of a small diesel engine. *Proc Instn Mech Engrs* 1974; 188: 253–261.
31. Wilson AR. The relative thickness of grease and oil films in rolling bearings. *Proc Instn Mech Engrs* 1979; 193: 185–192.
32. Sherrington I and Smith EH. Experimental methods for measuring the oil-film thickness between the piston-rings and cylinder-wall of internal combustion engines. *Tribol Int* 1985; 18: 315–320.
33. Chua WH and Stachowiak GW. The study of the dynamic thickness of organic boundary films under metallic sliding contact. *Tribol Lett* 2010; 39: 151–161.
34. Jablonka K, Glovnea R, Bongaerts J, et al. The effect of the polarity of the lubricant upon capacitance measurements of EHD contacts. *Tribol Int* 2013; 61: 95–101.
35. Sibley LB and Orcutt FK. Elasto-hydrodynamic lubrication of rolling-contact surfaces. *ASLE Trans* 1961; 4: 234–249.
36. Kirk MT. Hydrodynamic lubrication of ''Perspex''. *Nature* 1962; 194: 965–966.
37. Foord CA, Wedeven LD, Westlake FJ, et al. Optical elastohydrodynamics. *Proc Instn Mech Engrs* 1969; 184: 487–505.
38. Wedeven LD. *Optical measurements in elastohydrodynamic rolling contact bearing*. PhD Thesis, University of London, UK, 1970.

39. Kaneta M, Nishikawa H, Kameishi K, et al. Effects of elastic moduli of contact surfaces in elastohydrodynamic lubrication. *J Tribol* 1992; 114: 75.
40. Yagi K, Kyogoku K and Nakahara T. Experimental investigation of effects of slip ratio on elastohydrodynamic lubrication film related to temperature distribution in oil films. *Proc IMechE, Part J: J Engineering Tribology* 2006; 220: 353–363.
41. Cameron A and Gohar R. Theoretical and experimental studies of the oil film in lubricated point contact. *Proc R Soc A Math Phys Eng Sci* 1966; 291: 520–536.
42. Foord CA, Hamman WC and Cameron A. Evolution of lubricants using optical elastohydrodynamics. *ASLE Trans* 1968; 11: 31–43.
43. Westlake F and Cameron A. A study of ultra-thin lubricant films using an optical technique. *Proc Instn Mech Engrs* 1968; 182: 75–78.
44. Israelachvili J. Thin film studies using multiple-beam interferometry. *J Colloid Interface Sci* 1973; 44: 259–272.
45. Johnston GJ, Wayte R and Spikes HA. The measurement and study of very thin lubricant films in concentrated contacts. *Tribol Trans* 1991; 34: 187–194.
46. Guangteng G and Spikes HA. Boundary film formation by lubricant base fluids. *Tribol Trans* 1996; 39: 448–454.
47. Cann PM and Spikes HA. The behavior of polymer solutions in concentrated contacts: Immobile surface layer formation. *Tribol Trans* 2008; 37: 580–586.
48. Glovnea RP, Forrest AK, Olver AV, et al. Measurement of sub-nanometer lubricant films using ultra-thin film interferometry. *Tribol Lett* 2003; 15: 217–230.
49. Gustafsson L, Höglund E and Marklund O. Analysis, measuring lubricant film thickness with image. *Proc IMechE, Part J: J Engineering Tribology* 1994; 208: 199–205.
50. Cann PM, Spikes HA and Hutchinson J. The development of a spacer layer imaging method (SLIM) for mapping elastohydrodynamic contacts. *Tribol Trans* 1996; 39: 915–921.
51. Hartl M, Krupka I, Poliscuk R, et al. Thin film colorimetric interferometry. *Tribol Trans* 2001; 44: 270–276.
52. Chaomleffel J-P, Dalmaz G and Vergne P. Experimental results and analytical film thickness predictions in EHD rolling point contacts. *Tribol Int* 2007; 40: 1543–1552.
53. Luo J, Wen S and Huang P. Thin film lubrication. Part I. Study on the transition between EHL and thin film lubrication using a relative optical interference intensity technique. *Wear* 1996; 194: 107–115.
54. Guo F and Wong PL. A multi-beam intensity-based approach for lubricant film measurements in non-conformal contacts. *Proc IMechE, Part J: J Engineering Tribology* 2002; 216: 281–291.
55. Lauer JL and Peterkin ME. Analysis of infrared spectra of fluid films in simulated EHD contacts. *J Lubr Technol* 1975; 97: 145.
56. Lauer JL and Peterkin ME. Infrared emission spectra of elastohydrodynamic contacts. *J Lubr Technol* 1976; 98: 230.
57. Cann PM and Spikes HA. In lubro studies of lubricants in EHD contacts using FTIR absorption spectroscopy. *Tribol Trans* 1991; 34: 248–256.
58. Turchina V, Sanborn DM and Winer WO. Temperature measurements in sliding elastohydrodynamic point contacts. *J Lubr Technol* 1974; 96: 464.
59. Ausherman VK, Nagaraj HS, Sanborn DM, et al. Infrared temperature mapping in elastohydrodynamic lubrication. *J Lubr Technol* 1976; 98: 236.
60. Spikes HA, Anghel V and Glovnea R. Measurement of the rheology of lubricant films within elastohydrodynamic contacts. *Tribol Lett* 2004; 17: 593–605.
61. Yagi K, Kyogoku K and Nakahara T. Relationship between temperature distribution in EHL film and dimple formation. *J Tribol* 2005; 127: 658.
62. Reddyhoff T, Spikes HA and Olver AV. Improved infrared temperature mapping of elastohydrodynamic contacts. *Proc IMechE, Part J: J Engineering Tribology* 2009; 223: 1165–1177.
63. Long DA. *Raman spectroscopy*. New York: McGraw-Hill, 1977.
64. Ferraro JR, Nakamoto K and Brown CW. *Introductory Raman spectroscopy*. 2nd ed. San Diego: Academic Press, 2003.
65. Gardiner DJ, Baird E, Gorvin AC, et al. Raman spectra of lubricants in elastohydrodynamic entrapments. *Wear* 1983; 91: 111–114.
66. Gardiner DJ, Baird EM, Craggs C, et al. Raman microspectroscopy of a working elastohydrodynamic contact. *Lubr Sci* 1989; 1: 301–313.
67. LaPlant F, Laurence G and Ben-Amotz D. Theoretical and experimental uncertainty in temperature measurement of materials by Raman spectroscopy. *Appl Spectrosc* 1996; 50: 1034–1038.
68. Hutchinson EJ, Shu D, LaPlant F, et al. Measurement of fluid film thickness on curved surfaces by Raman spectroscopy. *Appl Spectrosc* 1995; 49: 1275–1278.
69. Jubault I, Mansot JL, Vergne P, et al. In situ pressure measurements using Raman microspectroscopy in a rolling elastohydrodynamic contact. *J Tribol* 2002; 124: 114–120.
70. Jubault I, Mansot JL, Vergne P, et al. In situ pressure measurements in an elastohydrodynmaically lubricated point contact using Raman microspectrometry. Comparison with numerical calculations. In: *Proceedings of 29th Leeds-Lyon symposium on tribology*, Leeds, vol. 41, 2003, pp.663–673.
71. Jubault I, Molimard J, Lubrecht AA, et al. In situ pressure and film thickness measurements in rolling/sliding lubricated point contacts. *Tribol Lett* 2003; 15: 421–429.
72. Vergne P and Ville F. Experimental investigation on the pressure distribution for pure sliding EHL contacts with dented surfaces. In: *IUTAM symposium on elastohydrodynamics and micro-elastohydrodynamics*, Solid Mechanics and its Applications, vol. 134, 2006, pp.201–213.
73. Yagi K, Vergne P and Nakahara T. In situ pressure measurements in dimpled elastohydrodynamic sliding contacts by Raman microspectroscopy. *Tribol Int* 2009; 42: 724–730.
74. Jabłoński A. Über den Mechanismus der Photolumineszenz von Farbstoffphosphoren. *Zeitschrift für Phys* 1935; 94: 38–46.
75. Smart AE and Ford RAJ. Measurement of thin liquid films by a fluorescence technique. *Wear* 1974; 29: 41–47.

76. Ford RAJ and Foord CA. Laser-based fluorescence techniques for measuring thin liquid films. *Wear* 1978; 51: 289–297.
77. Inagaki H, Saito A, Murakami M, et al. Development of two-dimensional oil film thickness distribution measuring system. *SAE Tech Pap* 1995; 952346.
78. Nakayama K, Morio I, Katagiri T, et al. A study for measurement of oil film thickness on engine bearing by using laser induced fluorescence (LIF) method. *SAE Tech Pap* 2003; 2003-01-0243.
79. Sugimura J, Hashimoto M and Yamamoto Y. Study of elastohydrodynamic contacts with fluorescence microscope. In: *Proceedings of 26th Leeds-Lyon symposium on tribology*, Leeds, vol. 38, 2000, pp.609–617.
80. Reddyhoff T, Choo JH, Spikes HA, et al. Lubricant flow in an elastohydrodynamic contact using fluorescence. *Tribol Lett* 2010; 38: 207–215.
81. Ponjavic A, Chennaoui M and Wong JSS. Through-thickness velocity profile measurements in an elastohydrodynamic contact. *Tribol Lett* 2013; 50: 261–277.
82. Davoust J, Devaux P and Leger L. Fringe pattern photobleaching: A new method for the measurement of transport coefficients of biological macromolecules. *EMBO J* 1982; 1: 1233–1238.
83. Bair S, Qureshi F and Winer WO. Observations of shear localization in liquid lubricants under pressure. *J Tribol* 1993; 115: 507–513.
84. Horvat FE and Braun MJ. Comparative experimental and numerical analysis of flow and pressure fields inside deep and shallow pockets for a hydrostatic bearing. *Tribol Trans* 2011; 54: 548–567.
85. Dwyer-Joyce RS, Drinkwater BW and Donohoe CJ. The measurement of lubricant-film thickness using ultrasound. *Proc R Soc A Math Phys Eng Sci* 2003; 459: 957–976.
86. Dwyer-Joyce RS, Reddyhoff T and Drinkwater BW. Operating limits for acoustic measurement of rolling bearing oil film thickness. *Tribol Trans* 2004; 47: 366–375.
87. Vetrone F, Naccache R, Zamarrón A, et al. Temperature sensing using fluorescent nanothermometers. *ACS Nano* 2010; 4: 3254–3258.
88. Jaque D and Vetrone F. Luminescence nanothermometry. *Nanoscale* 2012; 4: 4301–4326.
89. Cui Y, Xu H, Yue Y, et al. A luminescent mixed-lanthanide metal-organic framework thermometer. *J Am Chem Soc* 2012; 134: 3979–3982.
90. Wang X, Wolfbeis OS and Meier RJ. Luminescent probes and sensors for temperature. *Chem Soc Rev* 2013; 42: 7834–7869.
91. Christofferson J, Maize K, Ezzahri Y, et al. Microscale and nanoscale thermal characterization techniques. *J Electron Packag* 2008; 130: 41101.
92. Shi L, Kwon O, Miner AC, et al. Design and batch fabrication of probes for Sub-100 nm scanning thermal microscopy. *J Microelectromech Syst* 2001; 10: 370–378.
93. Liu W and Yang B. Thermography techniques for integrated circuits and semiconductor devices. *Sens Rev* 2007; 27: 298–309.
94. Christofferson J and Shakouri A. Thermal measurements of active semiconductor micro-structures acquired through the substrate using near IR thermoreflectance. *Microelectronics J* 2004; 35: 791–796.
95. Farzaneh M, Maize K, Lüerßen D, et al. CCD-based thermoreflectance microscopy: Principles and applications. *J Phys D Appl Phys* 2009; 42: 143001.
96. Csendes A, Székely V and Rencz M. Thermal mapping with liquid crystal method. *Microelectron Eng* 1996; 31: 281–290.
97. Choi CL, Koski KJ, Sivasankar S, et al. Strain-dependent photoluminescence behavior of CdSe/CdS nanocrystals with spherical, linear, and branched topologies. *Nano Lett* 2009; 9: 3544–3549.